

**Fe<sub>2</sub>O<sub>3</sub>-Mg-Al SUPPORTED BEADS FOR PHOSPHATE REMOVAL**



**Miss Chanyarak Watthanachai**

ศูนย์วิทยทรัพยากร  
จุฬาลงกรณ์มหาวิทยาลัย

**A Thesis Submitted in Partial Fulfillment of the Requirements  
for the Degree of Master of Science Program in Environmental Management**

**(Interdisciplinary Program)**

**Graduate School**

**Chulalongkorn University**

**Academic Year 2010**

**Copyright of Chulalongkorn University**

สารประกอบออกไซด์เหล็ก-แมกนีเซียม-อลูมิเนียม เคลือบบนเม็ดปิดสำหรับการกำจัดฟอสเฟต



นางสาว จรรย์รักษ์ วัฒนชัย

ศูนย์วิทยทรัพยากร

จุฬาลงกรณ์มหาวิทยาลัย

วิทยานิพนธ์นี้เป็นส่วนหนึ่งของการศึกษาตามหลักสูตรปริญญาวิทยาศาสตรมหาบัณฑิต

สาขาวิชาการจัดการสิ่งแวดล้อม (สหสาขาวิชา)

บัณฑิตวิทยาลัย จุฬาลงกรณ์มหาวิทยาลัย


ปีการศึกษา 2553

ลิขสิทธิ์ของจุฬาลงกรณ์มหาวิทยาลัย

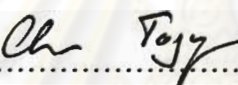
Thesis Title                      Fe<sub>2</sub>O<sub>3</sub>-Mg-Al SUPPORTED BEADS FOR PHOSPHATE  
REMOVAL  
By                                      Miss Chanyarak Watthanachai  
Field of Study                      Environmental Management  
Thesis Advisor                      Associate Professor Nurak Grisdanurak, Ph.D.

---

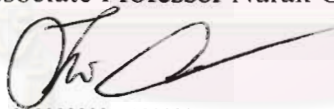
Accepted by the Graduate School, Chulalongkorn University in Partial  
Fulfillment of the Requirements for the Master's Degree


..........Dean of the Graduate School  
(Associate Professor Pornpote Piumsomboon, Ph.D.)


THESIS COMMITTEE

..........Chairman  
(Assistant Professor Chantira Tongcompou, Ph.D.)

..........Thesis Advisor  
(Associate Professor Nurak Grisdanurak, Ph.D.)

..........Examiner  
(Associate Professor Jin Anotai, Ph.D.)

..........Examiner  
(Patiparn Punyapalakul, Ph.D.)

..........External Examiner  
(Pongtanawat Khemthong, Ph.D.)

จรรยาวัชร วัฒนชัย : สารประกอบออกไซด์เหล็ก-แมกนีเซียม-อลูมิเนียม เคลือบบนเม็ด  
 บีดสำหรับการกำจัดฟอสเฟต ( $\text{Fe}_2\text{O}_3$ -Mg-Al SUPPORTED BEADS FOR PHOSPHATE  
 REMOVAL) อ. ที่ปริกษาวิทยานิพนธ์หลัก: รศ.ดร. นุรักษ์ กฤษดานุรักษ์, 63 หน้า.

การกำจัดฟอสเฟตด้วยกระบวนการดูดซับ โดยใช้ Layered Double Hydroxides (LDH) ปรับสภาพด้วยสารประกอบแมกนีเซียม-อลูมิเนียม และสารประกอบแมกนีเซียม- อลูมิเนียมที่เติม ออกไซด์เหล็ก ซึ่งตัวดูดซับได้ถูกสังเคราะห์จากกระบวนการการตกตะกอนร่วมภายใต้อัตราส่วน 2:1 และ 0.05:2:1 โดยมวลของสารประกอบแมกนีเซียม-อลูมิเนียม และออกไซด์เหล็ก-แมกนีเซียม-อลูมิเนียมตามลำดับ จากนั้นจึงวิเคราะห์คุณลักษณะทางกายภาพด้วยเทคนิคการ เลี้ยวเบนของรังสีเอกซ์ การดูดซับ- คายซ้ำของก๊าซไนโตรเจนกล่องจุลทรรศน์อิเล็กตรอนแบบส่อง กราด เอกซเรย์ฟลูออเรสเซนส์ และฟูเรียร์ทรานส์ฟอร์มอิน ฟาเรด พบว่าสาร ประกอบออกไซด์ เหล็กสามารถเพิ่มพื้นที่ผิวของตัวดูดซับและเพิ่มความสามารถในการดูดซับฟอสเฟตได้ คือ 31 มิลลิกรัมฟอสฟอรัสต่อกรัมตัวดูดซับ สอดคล้องกับไอโซเทิร์มแบบแลงเมียร์ ขณะที่จลนศาสตร์การ ดูดซับสามารถอธิบายด้วยปฏิกิริยาอันดับสองเทียบเท่ากับความสัมพันธ์ของฟอสเฟต และเพื่อ ความสะดวกในการนำไปใช้สำหรับการบำบัดน้ำเสียจริง จึงได้มีการศึกษาการขึ้นรูปเป็นเม็ดด้วย วิธีการเคลือบเชิงกลและการอัดฉีด พบว่าตัวดูดซับด้วยวิธีการเคลือบเชิงกลมีความสามารถในการ ดูดซับฟอสเฟตได้ดีกว่าวิธีการอัดฉีด ดังนั้นสารประกอบออกไซด์เหล็ก- แมกนีเซียม-อลูมิเนียมทั้ง แบบเม็ดและผง สามารถเป็นตัวเลือกหนึ่งในการดูดซับฟอสเฟตในน้ำได้เป็นอย่างดี

## ศูนย์วิทยทรัพยากร จุฬาลงกรณ์มหาวิทยาลัย

สาขาวิชา การจัดการสิ่งแวดล้อม

ลายมือชื่อนิสิต

จันทวัชร วัฒนชัย

ปีการศึกษา 2553

ลายมือชื่อ อ.ที่ปริกษาวิทยานิพนธ์หลัก

*[Signature]*

# # 5287536020 : MAJOR ENVIRONMENTAL MANAGEMENT

KEYWORDS : ADSORPTION/ PHOSPHATE/ LAYERED DOUBLE  
HYDROXIDES/ CO-PRECIPIATION

CHANYARAK WATTHANACHAI: Fe<sub>2</sub>O<sub>3</sub>-Mg-Al SUPPORTED BEADS  
FOR PHOSPHATE REMOVAL. ADVISOR: ASSOC. PROF. NURAK  
GRISDANURAK, Ph.D., 63 pp.

The phosphate removal in surface water by adsorption on Mg-Al LDHs and Fe<sub>2</sub>O<sub>3</sub>-Mg-Al LDHs or layered double hydroxides was investigated. The materials were synthesized by co-precipitation method in and 2:1 and 0.05:2:1 weight ratio as Mg-Al and Fe<sub>2</sub>O<sub>3</sub>-Mg-Al, respectively. Their structure formed in layered double hydroxides (LDHs) was confirmed by XRD, SEM, XRF, FT-IR and BET specific surface area. The introduction of Fe<sub>2</sub>O<sub>3</sub> into the main structure increased the specific surface area and affected the phosphate adsorption capacity. Based on Langmuir isotherm, 31 mg P/g Fe<sub>2</sub>O<sub>3</sub>-Mg-Al LDHs was observed. Adsorption kinetic followed pseudo-second-order kinetic model with respect to phosphate concentration. The synthesized materials were applied to the fabrication of granular adsorbent for use in the wastewater treatment. The phosphate adsorption capacity obtained by material via mechanical coating was higher than that using extrusion technique. In conclusion, both types (powder and pellet) of Fe<sub>2</sub>O<sub>3</sub>-Mg-Al LDHs could be an alternative material for the removal of phosphate for the surface water.

ศูนย์วิทยทรัพยากร  
จุฬาลงกรณ์มหาวิทยาลัย

Field of Study: Environmental Management

Academic Year: 2010

Student's Signature Chanyarak Watthannachai

Advisor's Signature Nurak Grisdanurak

## ACKNOWLEDGEMENTS

The achievement of this thesis can be completed with several assistances. I, therefore, would like to give the sincere appreciation to these people, as follows;

First of all, I would like to convey the greatest appreciate to my advisor, Associate Professor Dr. Nurak Grisdanurak, who gave me suggestions, knowledge, attention and experience to complete the work.

The thankfulness is also for the thesis committee chairman, Assistant Professor Dr. Chantra Tongcompou, and the thesis committee members, Associate Professor Dr. Jin Anotai, Dr. Patiparn Punyapalakul and Dr. Pongtanawat Khemthong, for the useful suggestions. Special thanks are towards Dr. Jilada Chumee, Kitirote Wantala and Laksana Laokiat for suggesting and improving of my knowledge in this thesis and laboratory. Moreover, this study was refunded and supported by National Center of Excellence for Environmental and Hazardous Waste Management (NCE-EHWM) and the Graduate Program of Chulalongkorn University

Thank you for unconditioned encouragement from my parents, and friends in Thammasat University (Faculty of Chemical Engineering) and in Chulalongkorn University (NCE-EHWM).



ศูนย์วิทยทรัพยากร  
จุฬาลงกรณ์มหาวิทยาลัย

# CONTENTS

	<b>Page</b>
ABSTRACT (Thai).....	iv
ABSTRACT (English).....	v
ACKNOWLEDGEMENTS.....	vi
CONTENTS.....	vii
LIST OF TABLES.....	ix
LIST OF FIGURES.....	x
LIST OF ABBREVIATIONS.....	xii
CHAPTER I INTRODUCTION.....	1
1.1 Background.....	1
1.2 Objectives.....	2
1.3 Hypothesis.....	2
1.4 Scopes of the study.....	2
CHAPTER II BACKGROUND AND LITERATURE REVIEWS.....	3
2.1 Phosphate.....	3
2.2 Principle of adsorption.....	6
2.2.1 Types of adsorption.....	6
2.2.2 Factors influencing adsorption.....	7
2.2.3 Adsorption isotherm.....	8
2.2.3.1 Langmuir adsorption isotherm.....	8
2.2.3.2 Freundlich adsorption isotherm.....	9
2.3 Adsorbent for phosphate adsorption.....	9
2.3.1 Layered double hydroxides.....	11
2.4 Granular formation of adsorbent.....	13
2.4.1 Mechanical coating.....	13
2.4.2 Extrusion.....	14
CHAPTER III METHODOLOGY.....	16
3.1 Chemical and apparatus.....	16

	<b>Page</b>
3.1.1 Chemical.....	16
3.1.2 Apparatus.....	16
3.2 Experimental procedures.....	17
3.2.1 Preparation of phosphate solution.....	17
3.2.2 Material synthesis.....	18
3.3.3 Granular formation of sample.....	19
3.3.3.1 Mechanical coating.....	19
3.3.3.2 Extrusion.....	20
3.3.4 Adsorption studies.....	21
3.4 Analytical methods.....	22
3.4.1 Characterization.....	22
3.4.2 Analysis.....	23
<b>CHAPTER IV RESULTS AND DISCUSSION.....</b>	<b>24</b>
4.1 Powder form of adsorbent.....	24
4.1.1 Characterizations.....	24
4.1.2 Adsorption capacity.....	29
4.1.3 Kinetic study.....	35
4.2 Granular form of adsorbents.....	38
4.2.1 Surface area.....	38
4.2.2 Phosphate adsorption.....	39
<b>CHAPTER V CONCLUSIONS AND RECOMMENDATIONS.....</b>	<b>41</b>
5.1 Conclusions.....	41
5.2 Recommendations.....	42
<b>REFERENCES.....</b>	<b>43</b>
<b>APPENDIX.....</b>	<b>48</b>
<b>BIOGRAPHY.....</b>	<b>63</b>



## LIST OF TABLES

Table		Page
2.1	Properties of phosphate.....	4
2.2	Examples of phosphate removal techniques and their proc/cons...	5
2.3	Properties of the emulsion copolymer of pure acrylic .....	15
4.1	Chemical compositions of prepared materials.....	28
4.2	BET surface areas of adsorbents.....	28
4.3	Langmuir and Freundlich constants .....	33
4.4	Pseudo-first-order and pseudo-second-order kinetic model.....	38
4.5	BET surface areas of granular adsorbents.....	39
(1)	C/C <sub>0</sub> of phosphate using Fe <sub>2</sub> O <sub>3</sub> -Mg-AlLDHs.....	49
(2)	C/C <sub>0</sub> of phosphate using Mg-Al LDHs.....	50
(3)	Adsorption capacity of Fe <sub>2</sub> O <sub>3</sub> -Mg-Al LDHs.....	51
(4)	Adsorption capacity of Mg-Al LDHs.....	52
(5)	Percentage of adsorption of Fe <sub>2</sub> O <sub>3</sub> -Mg-Al LDHs.....	53
(6)	Percentage of adsorption of Mg-Al LDHs.....	54
(7)	Langmuir adsorption isotherm of adsorbents.....	55
(8)	Separate factor (R <sub>L</sub> ).....	56
(9)	Freundlich adsorption isotherm of adsorbents.....	57
(10)	Pseudo-first-order and pseudo-second-order kinetic model.....	58
(11)	Concentration of phosphate using mechanical coating .....	60
(12)	Concentration of phosphate using extrusion.....	61
(13)	Percentage of adsorption of granular adsorbents by mechanical coating and extrusion.....	62

## LIST OF FIGURES

Figure		Page
2.1	Speciation diagram of phosphate .....	5
2.2	Structure of LDHs.....	12
2.3	Mechanical coating features .....	14
2.4	Extrusion process.....	14
3.1	Experimental schemes of this work.....	17
3.2	Procedure of Fe <sub>2</sub> O <sub>3</sub> -Mg-Al LDHs synthesis.....	18
3.3	Preparation of granules by mechanical coating.....	19
3.4	Preparation of Fe <sub>2</sub> O <sub>3</sub> granules by extrusion.....	20
3.5	Phosphate adsorption testing procedure.....	21
4.1	XRD patterns of Fe <sub>2</sub> O <sub>3</sub> -Mg-Al LDHs, Mg-Al LDHs and LDHs .....	25
4.2	SEM micrographs of Fe <sub>2</sub> O <sub>3</sub> -Mg-Al LDHs, Mg-Al LDHs and LDHs.....	26
4.3	FT-IR spectrum of Fe <sub>2</sub> O <sub>3</sub> -Mg-Al LDHs and Mg-Al LDHs.....	27
4.4	Concentration profile of remained phosphate in the solution over Fe <sub>2</sub> O <sub>3</sub> -Mg-Al LDHs and Mg-Al LDHs.....	29
4.5	Sorption of phosphate on Fe <sub>2</sub> O <sub>3</sub> -Mg-Al LDHs and Mg-Al LDHs .....	31
4.6	Linearization of the plot; Langmuir and Freundlich isotherm.....	32
4.7	Separation factors (R <sub>L</sub> ).....	34
4.8	Linear plots of pseudo-first-order kinetic model on both adsorbents.....	36
4.9	Linear plots of pseudo-second-order kinetic model on both adsorbents.....	36
4.10	Percentage of phosphate adsorption on granulated adsorbents.....	40
(1)	C/C <sub>0</sub> of phosphate using Fe <sub>2</sub> O <sub>3</sub> -Mg-Al LDHs.....	49
(2)	C/C <sub>0</sub> of phosphate using Mg-Al LDHs.....	50
(3)	Adsorption capacity of Fe <sub>2</sub> O <sub>3</sub> -Mg-Al LDHs.....	51
(4)	Adsorption capacity of Mg-Al LDHs.....	52

	Page
(5) Percentage of adsorption of Fe <sub>2</sub> O <sub>3</sub> -Mg-Al LDHs.....	53
(6) Percentage of adsorption of Mg-Al LDHs.....	54
(7) Linear plots of Langmuir adsorption isotherm of adsorbents.....	55
(8) Separate factor (R <sub>L</sub> ).....	56
(9) Linear plots of Freundlich adsorption isotherm of adsorbent.....	57
(10a) Linear plot of pseudo-first-order kinetic model .....	58
(10b) Linear plot of pseudo-second-order kinetic model.....	59
(11) Concentration of phosphate using mechanical coating.....	60
(12) Concentration of phosphate using extrusion.....	61
(13) Percentage of adsorption of granular adsorbents by mechanical coating and extrusion.....	62



ศูนย์วิทยทรัพยากร  
 จุฬาลงกรณ์มหาวิทยาลัย

## LIST OF ABBREVIATIONS

$^{\circ}\text{C}$	Degree of Celsius
$\lambda$	Lambda
cm	Centimeter
$\mu\text{m}$	Micrometer
mm	Millimeter
nm	Nanometer
m	Meter
$\Theta$	Theta
g	Gram
h	Hour
min	Minute
l	Liter
Kg	Kilogram
mA	Miliampere
mg	Milligram
ml	Milliliter
M	Molar
K	Degree of Kelvin
P	Phosphorus
$\text{PO}_4^{3-}$	Phosphate
LDHs	Layered double hydroxides
Al	Aluminium
$\text{Al}^{3+}$	Aluminium ion
$\text{Al}_2\text{O}_3$	Aluminium (III) oxide
$\text{Al}(\text{NO}_3)_3 \cdot 9\text{H}_2\text{O}$	Aluminium nitrate
Mg	Magnesium
$\text{Mg}^{2+}$	Magnesium ion
MgO	Magnesium oxide
$\text{Mg}(\text{NO}_3)_2 \cdot 6\text{H}_2\text{O}$	Magnesium nitrate
$\text{Fe}^{3+}$	Ferric ion (Iron ion)
$\text{Fe}_2\text{O}_3$	Ferric oxide

$\text{Fe}(\text{NO}_3)_3 \cdot 9\text{H}_2\text{O}$	Ferric nitrate
$\text{Na}_2\text{CO}_3$	Sodium carbonate
$\text{NaOH}$	Sodium hydroxide
$\text{KH}_2\text{PO}_4$	Dihydrogen orthophosphate
$(\text{NH}_4)_6\text{Mo}_7\text{O}_{24} \cdot 4\text{H}_2\text{O}$	Ammonium molybdate
$\text{NH}_4\text{VO}_3$	Ammonium metavanadate
$\text{HNO}_3$	Nitrite acid
$\text{HCl}$	Hydrochloric acid



ศูนย์วิทยทรัพยากร  
จุฬาลงกรณ์มหาวิทยาลัย

# CHAPTER I

## INTRODUCTION

### 1.1 Background

Eutrophication is the process by which a water body obtains a high concentration of nutrient, especially phosphates. It could stimulate the growth of aquatic plant and lives, usually resulting in the depletion of dissolve oxygen (DO). Thus, phosphate is the main cause of eutrophication that effects to the water quality. EPA water quality has set criteria for phosphate concentration in several suitable the concentration should not exceed 0.05 mg/l for the discharge steam into any reservoirs. It is set of 0.025 mg/l within a lake or reservoirs and 0.1 mg/l in streams or flowing water to control algae growth (USEPA, 1986). Phosphate contaminated sources have been concerned in both pre- and post-releases. There are many phosphate removal techniques chemical precipitation, crystallization, reverse osmosis and adsorption. The adsorption technology is applied in this study. Therefore, the focus is to search for the suitable adsorbent.

Many adsorbents such as fly ash (Chen et al., 2006), blast furnace slag, zeolite and titanium oxide (Ozacar, 2003), activated alumina and granulated ferric hydroxide (Genz et al., 2004), iron oxide tailing (Zeng et al., 2004), modified palygorskites (aluminium-magnesium silicate) (Ye et al., 2006), red mud (Akay et al., 1998) and layered double hydroxides (LDHs) (Das et al. 2006; Miyauchi et al., 2009) have been widely applied for phosphate adsorption. Among them, Mg-Al LDHs effective was found to be in phosphate removal. It was also claimed that the technique is in low investment. Layered double hydroxides (LDH) are also known as anionic clay or hydrotalcite-like-compounds. It has high anion-exchange capacities and flexible interlayer spaces. LDHs are synthesized by co-precipitation method at constant pH.10 which consists of precipitation, aging, washing/filtration, drying and calcinations.

The obtained adsorbent is in powder form. To prevent the clogging during the use and able to reuse granular form is also tested. In this study, the granular formation by mechanical coating (Yoshida et al., 2009) and extrusion technique (Haba and Narkis, 2003) are implemented.

$\text{Fe}_2\text{O}_3$  was selected to modify Mg-Al LDHs, to higher phosphate adsorption. The co-precipitation is still used.

## 1.2 Objectives

The main purpose of this study is to synthesize and fabricate of  $\text{Fe}_2\text{O}_3$ -Mg-Al LDHs supported bead for phosphate removal. Two sub-objectives of this study are as follows;

- To synthesize and characterize  $\text{Fe}_2\text{O}_3$ -Mg-Al LDHs supported beads.
- To study the reliability of  $\text{Fe}_2\text{O}_3$ -Mg-Al in application of phosphate adsorption.

## 1.3 Hypothesis

$\text{Fe}_2\text{O}_3$  enhances the adsorption efficiency of phosphate over Mg-Al LDHs in both powder and granular forms.

## 1.4 Scope of the study

1.  $\text{Fe}_2\text{O}_3$ -Mg-Al LDHs and Mg-Al LDHs samples are prepared by using co-precipitation method.
  - The molar ratio of  $\text{Fe}_2\text{O}_3$ : Mg: Al LDHs and Mg: Al LDHs is 0.05:2:1 and 2:1, respectively.
  - The study is constant carried out pH of 10.
  - The calcination temperature is at  $550^\circ\text{C}$  for 6 h.
2. The phosphate solution is prepared in laboratory with initial concentrations of 1, 5, 10, 20, 30 and 40 mg P/l.

## CHAPTER II

### BACKGROUND AND LITERATURE REVIEWS

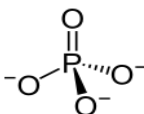
#### 2.1 Phosphate

Phosphate is the common form of the element phosphorus and essential nutrient for all life. Although, it is the nutrient for the growth of organism in most ecosystems, the increased nutrient concentrations cause eutrophication. It is the process of increasing organic enrichment and is accelerated by input of excessive phosphate including an accelerated plant growth, algal blooms, low dissolved oxygen and the death of aquatic animals (USEPA, 1986). Moreover, harmful algal blooms (e.g. *cyanobacteria* and *pfisteria*) can also cause the mortality in animal and human. There are many sources of phosphate, both natural and human including rock and soil, wastewater treatment plants, runoff from farm fertilizer, disturbed land areas, commercial cleaning and laundries productions. The EPA water quality had set the standards, as mentioned previously.

Phosphate is denoted as  $\text{PO}_4^{3-}$  in tetrahedral structure. The properties of phosphate are shown in Table 2.1. In nature, phosphates have three forms including orthophosphate, metaphosphate (polyphosphate) and organic phosphate. Each form contains phosphate in different chemical formulas. Orthophosphate forms are produced by natural process (e.g. freshwater and marine system) and found in wastewater. Polyphosphate forms are used for treating boiler water and in detergents, which can change to the “ortho” form in water. The last form is organic phosphates that are important in nature and also may effect in the breakdown of organic pesticides containing phosphates. In the field of chemically based, compounds for monitoring phosphate depending on measuring orthophosphate.



**Table 2.1** Properties of phosphate

Molecular formula	 $\text{PO}_4^{3-}$
MSDS number	P3902
Appearance	Clear, colorless, solution, odorless
Molecular weight	94.97
Solubility	Miscible in water
Specific Gravity	1
pH	No information found
Boiling point	100 °C
Melting point	0 °C
Health and Environmental effect	High levels of $\text{PO}_4^{3-}$ are toxic to people or animal.

Phosphates ion present in a polyatomic ion. It can be separated in four forms regarding to the pH of the solution, including (Chang, 2006), present in Figure 2.1.

- The phosphate ion ( $\text{PO}_4^{3-}$ ) predominates in strongly basic conditions.
- The hydrogen phosphate ion ( $\text{HPO}_4^{2-}$ ) is prevalent in weakly basic conditions.
- The dihydrogen phosphate ion ( $\text{H}_2\text{PO}_4^-$ ) is common in weakly acid conditions.
- Aqueous phosphoric acid ( $\text{H}_3\text{PO}_4$ ) is the main form in strong acid.

จุฬาลงกรณ์มหาวิทยาลัย

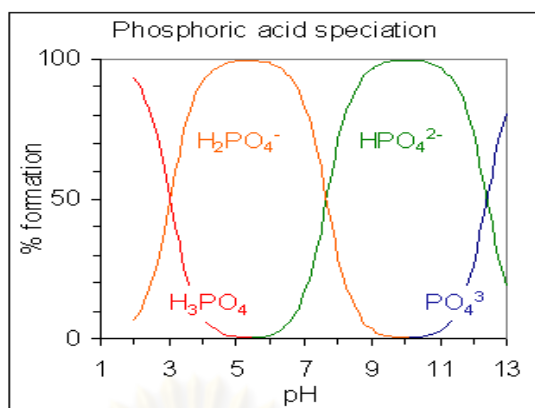


**Figure 2.1** Speciation diagram of phosphate.

There are many techniques for phosphate removal from aquatic system, using widely as physical, chemical (or physical-chemical) and biological techniques. Advantages and disadvantages for each technique are listed in Table 2.2. Most method is not cost effective and not suitable for application on a household scale. Among them adsorption technology can be applied in small devices and is appropriate on household scale. In next sections, the details adsorption and adsorbent will be discussed.

**Table 2.2** Examples of phosphate removal techniques and their pros/cons

Technique	Method	Advantage	Disadvantage
Physical	Filtration	Easy operation and suitable for suspended solids removal.	Difficult of handling.
	Precipitation (Bashan et al., 2004).	Easy operation and easily available materials.	More sludge production & complex a small scale.
Chemical	Adsorption (Chitrakar et al., 2006)	Low cost, easily available materials, less production of sludge, easy operation.	Clogs the adsorbent bed and difficult of handling.
Biological	Bio-bacteria (Yildiz, 2004)	Suitable for removal a phosphate compounds.	Use a long time for a reaction.

## 2.2 Principle of adsorption

Adsorption is a process of forming an atomic or molecular film (adsorbate) that occurs when a gas or liquid solute to accumulate on a solid or liquid surface (adsorbent). It is different from absorption, in which a dispersion of substance into a liquid is or solid to generates a solution that form a new chemical species at the exposed surface. The term sorption surround both processes, while desorption is the reverse process (Faust and Aly, 1998).

### 2.2.1 Types of adsorption

Adsorption is usually applied for physical, chemical, and biological systems and it is well-known in industrial operation. In addition, the adsorption is typically used in wastewater treatment to remove toxic substances from wastewater. Normally, the adsorption is found in the tertiary wastewater treatment as a polishing step before discharge. Adsorption can be classified into two categories as follows (Grisdanurak and Wittayakun, 2004);

- Physical adsorption is process in which the force of attraction between the molecules of the adsorbate and the adsorbent are the van der Waals force. The interaction energy is very weak. The physical adsorption depends on the surface area of the adsorbent and the nature of the adsorbate. Moreover, it is favored at low temperature. The physical adsorption process can be reversed by heating or decreasing the pressure of the adsorbate. So, the physical adsorption is several layers thick (multilayer).
- Chemical adsorption is process in which the force of attraction between the adsorbate and the adsorbent are very strong. The molecules of adsorbate are formed with chemical bonds (e.g. covalent and ionic bonds) on the surface of the adsorbent. The chemical adsorption depends on the nature of the adsorbent and adsorbate, while it occurs usually at high temperature. So, the surface in chemical adsorption is covered by a single layer of the adsorbates (monolayer).

### 2.2.2 Factors influencing adsorption

Solids have a tendency to adsorb liquids or gases to satisfy the unsatisfied valences on their surface. The important factors that influence adsorption of liquids or gases on solids are the following (Akewaranugulsiri, 2008)

- Surface area and pore size of adsorbents
- Particle size
- Chemistry of the surface
- Nature of adsorbate and adsorbent
- Effect of temperature
- Effect of pressure

In both types of adsorption, the amount of gas adsorbed at an initially increased temperature with increase in pressure, so it becomes constant at high pressure. However, pressure effect is not an issue for liquid-solid adsorption.

In addition, several models and parameters are described to investigate and understand involve the adsorption behaviors. The parameters are widely used to explain the efficiency and capacity of adsorption as following;

- **The percentage of adsorption** of adsorbed ions on adsorbent is calculated according to:

$$\text{Percent adsorption} = \frac{(C_0 - C)100}{C_0}$$

- **The adsorption capacity** of adsorbent is the amount of adsorbed substance reached in a saturated solution or strongly adsorbed solutes of limited solubility. It is calculated in unit of mg/g adsorbent, according to (IUPAC, 1997):

$$\text{Adsorption capacity} = \frac{(C_0 - C)V}{W}$$

### 2.2.3 Adsorption isotherm

Adsorption is usually described through isotherms, that is a function of the amount of adsorbate on the adsorbent, related to its pressure (if gas) or concentration (if liquid). The model describing process of adsorption takes the form of one of the following isotherms.

#### 2.2.3.1 The Langmuir adsorption isotherm

The Langmuir adsorption isotherm was published in 1916 by Irving Langmuir, and it is generally modifiable to chemisorptions. Moreover, it was originally derived from kinetic consideration, the basis of statistical mechanics and thermodynamics etc. The Langmuir adsorption isotherm can be assumed as reversible adsorption and desorption of the adsorbate molecules. It represents well data for single components based on four hypotheses; (Cussler, 1997)

1. The surface of the adsorbent is uniform that is all the adsorption sites are equal.
2. Adsorbed molecules do not interact.
3. All adsorption occurs through the same mechanism.
4. At the maximum adsorption, only a monolayer is formed molecules of adsorbate do not deposit on others, already adsorbed, molecules of adsorbate, only on the free surface of the adsorbent.

In addition, the adsorbed molecules (adsorbate) on solids (adsorbent), the Langmuir adsorption isotherm can be expressed in equation 1 (Boujelben et al., 2007);

$$q_e = \frac{bqC_e}{1 + qC_e} \quad (1)$$

and linearized to

$$\frac{C_e}{q_e} = \frac{1}{qb} + \frac{C_e}{q} \quad (2)$$

Where  $C_e$  is the equilibrium adsorption concentration in solution (mg/l),  $q_e$  denotes the amount adsorbed per unit mass of adsorbent (mg/g),  $b$  denote a constant related to affinity of the binding sites (l/mg) and  $q$  is the maximum adsorption capacity (mg/g) The data are fitted well by the Langmuir equation as shown by the regression

coefficient value. The value of  $b$  and  $q$  were determined from the slopes and intercepts of the straight-line plot between  $C_e$  and  $C_e/q_e$ .

### 2.2.3.2 The Freundlich adsorption isotherm

The Freundlich adsorption isotherm was published in 1894 by Freundlich and Küster, and is an empirical formula for gaseous adsorbates and can be used also for mixtures of compounds. Moreover, the Freundlich adsorption isotherm is generally modifiable to physisorption. The Freundlich equation can be mathematically represented by equation 2 (Boujelben et al., 2007).

$$q_e = K_F C_e^{1/n} \quad (3)$$

and linearized to

$$\log q_e = \log K_F + \frac{1}{n} \log C_e \quad (4)$$

Where  $q_e$  is the amount adsorbed per unit mass of adsorbent (mg/g),  $C_e$  is the equilibrium adsorption concentration in solution (mg/l),  $n$  and  $K_F$  is constant related to energy and intensity of adsorption and the adsorption capacity of the adsorbent. For linearization of data, the Freundlich equation is plotted between  $\log C_e$  and  $\log q_e$  in a straight line. The value  $K_F$  and  $n$  as calculated from the slopes and intercepts.

## 2.3 Adsorbent for phosphate adsorption

There are many adsorbents for phosphate adsorption such as fly ash (Chen et al., 2006), blast furnace slag, zeolite and titanium oxide (Ozacar, 2003), activated alumina and granulated ferric hydroxide (Genz et al., 2004), iron oxide tailing (Zeng et al., 2004), modified palygorskites (aluminium-magnesium silicate) (Ye et al., 2006), red mud (Akay et al., 1998) and layered double hydroxides (LDHs) (Das et al., 2006; Miyauchi et al., 2009). In addition, other adsorbents made from agricultural residues such as modified whet residue (Xu et al., 2009) and coconut husk (Manju et al., 1998). Many adsorbents regarding to the resource of materials that can be classified as waste materials or by-products, commercial materials, agricultural residues and natural materials.

However, these wastes or by-products are hardly used in application due to their low and unstable adsorption capacities to phosphate (Namasivayam and Prathap,

2005). The iron oxide tailing is one of waste tailing which it may be effective in removing soluble phosphate. The result showed that phosphate adsorption capacity tended to decrease with an increase of pH was 7 mgP/g tailing at pH 6.7 and desorbability of phosphate is 13-14%, which the waste tailing contained more than 30% iron oxides.

In addition, the application of easily available materials for phosphate adsorption such as activated aluminium oxide (AA), granulated ferric hydroxide (GFH) (Genz et al., 2004) and modified palygorskites (Ye et al., 2006). Although most materials are commercial adsorbent that has a high adsorption capacity, but the materials price for the adsorptive treatment is high cost. The commercial adsorbents as activated aluminium oxide and granulated ferric hydroxide were used for phosphate adsorption in membrane bioreactors (MBR) filtrates. GFH showed a higher maximum capacity and high affinity at low phosphate concentration compared to AA at pH 5.5, was 12.3 mg/g GFH and 7.9 mg/g AA.

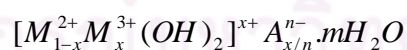
For modified palygorskites is an aluminum-magnesium silicate and has a fibrous morphology, which can be characterized as high surface areas and porosity, thermal resistance, and chemical inertness. Therefore, the structure of palygorskites is attractive adsorbent. The natural and modified palygorskites are located in China that was applied to remove phosphate from aqueous solutions (Ye et al., 2006). The modified palygorskites were prepared by activated with hydrochloric acid and/or thermal treatment. The result showed that modified palygorskites had faster kinetics and higher adsorption capacities than the natural palygorskites at equilibrium pH 7.0 was 9 mg P/g and 4 mg P/g, respective and the desorbability of phosphate is 10-13%.

For Mg-Al-LDHs, that is well-known as hydrotalcite-like-compounds (HTLcs) or anionic clays have been widely applied as adsorbents. LDHs proved to be an interesting material for the removal of anionic surfactant (as phosphate) because it has low cost and high potential to clean up laundry leaching in water (Schouten et al., 2007). Generally, LDHs consist of positively charged mixed metal hydroxide sheets are separated by anionic ions ( $A^-$ ) and water molecules (You et al., 2001). Thus, it has high anion exchange capacities to remove phosphate from aqueous solution (Miyauhi et al., 2009; Das et al., 2006).

Various LDHs for phosphate adsorption in aqueous solution such as Mg-Al, Zn-Al, Ni-Al, Co-Al, Mg-Fe, Zn-Fe, Ni-Fe and Co-Fe was studied (Das et al., 2006). Mg-Al LDH with Mg/Al molar ratio of 2.0 showed higher adsorption capacity compared to other LDHs, which it possessed higher  $Al^{3+}$  content (Cosimo et al., 1998). However, Mg-Al LDHs have weak interlayer bonding as a result present expanding properties. Therefore, an attracted in the LDHs, which the brucite-like layers may impose an interlayer guests leading to enhanced control of rate of reaction and product distributions. A few reports have focused on the use of LDHs as precursors to mixed oxide formed that have specific properties, such as homogenous distribution of metal cation at the atomic level, high surface areas and high thermal stability (Vulic et al., 2008; Kishore and Rodrihues, 2008; Miyauchi et al., 2009). Iron ( $Fe^{3+}$ ) is one of the M(III) ion was mixed into Mg-Al LDHs. Due to high concentration of M(III) ion affect to increased the number of neighboring M(III) and leads to the formation of additional M(III)-hydroxide phase and formation of complex, multi-phase systems with specific structural and surface properties. The relation of increases the surface area and the small amount of iron was 5 mol% in ternary mixed oxides of Mg-Al-Fe series (Vulic et al., 2008). Although these adsorbents have effective phosphate adsorption capacity, most of them are not use in a solution under neutral pH conditions. The LDHs can effectively adsorb phosphate under pH 5.5-9 (Kindaichi et al., 2002). Therefore, the LDHs are investigated in this study.

### 2.3.1 Layered double hydroxides (LDHs)

LDHs are also known as anionic clay minerals or hydrotalcite-like-compound. The general formula of LDHs is (Cosimo et al., 1998);



Where  $M^{2+}$  is a divalent metal ion, such as  $Ca^{2+}$ ,  $Mg^{2+}$ ,  $Zn^{2+}$ ,  $Co^{2+}$ ,  $Ni^{2+}$ ,  $Cu^{2+}$ ,  $Mn^{2+}$  etc,  $M^{3+}$  is a trivalent metal ion, such as  $Al^{3+}$ ,  $Cr^{3+}$ ,  $Fe^{3+}$ ,  $Co^{3+}$ ,  $Mn^{3+}$ , etc and  $A^{n-}$  is an anion, such as  $Cl^-$ ,  $NO_3^-$ ,  $ClO_4^-$ ,  $CO_3^{2-}$ ,  $SO_4^{2-}$  etc, as shown in Figure 2.2 . The anions possess the interlayer region of these layered crystalline materials. The value of x is equal to the molar ratio of  $M^{2+}/(M^{2+} + M^{3+})$  which is obtained in a limited range as  $0.2 < x < 0.33$  (Cavani et al., 1991).



The structure of LDHs contains brucite-like layers and interlayer. Brucite consists of a hexagonal close packing of hydroxyl ions alternate with octahedral sites occupied by  $Mg^{2+}$  ions. The metal hydroxide sheets in brucite crystal are neutral in charge and stack up against another by Van der Waal's interaction. In LDHs, these brucite-like sheets are a substitution region of divalent by trivalent cation and the mixed metal hydroxide layers,  $[M_{1-x}^{2+}M_x^{3+}(OH)_2]^{x+}$  thus the formation obtained a net positive charge. This increasing charge on the metal hydroxide layers is neutralized with the anion accumulated in the interlayer region. Interlayer region in LDHs contains both anions and some water molecules for the stabilization of the crystal structure. The presence of the anion and water molecules leads to the expansion of the basal spacing from 0.48 nm (brucite) to 0.77 nm in LDH.

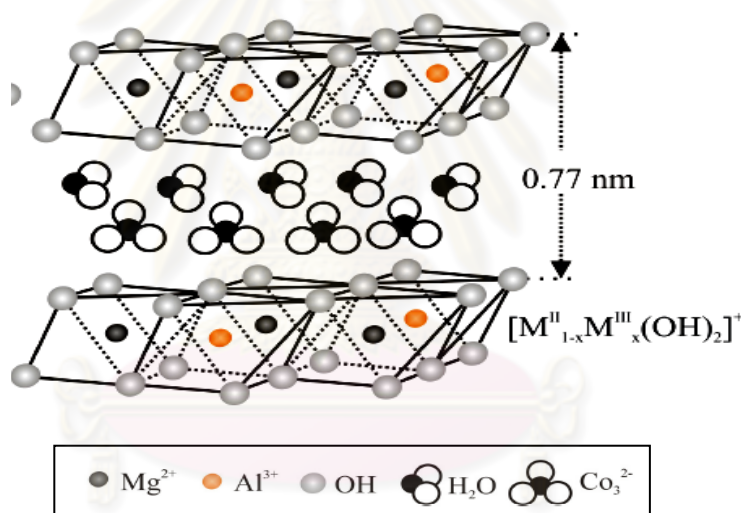


**Figure 2.2** Structure of LDHs consists of  $M^{(2+)} = Ca^{2+}, Mg^{2+}, Zn^{2+}, Ni^{2+}, Cu^{2+}$ , etc;  $M^{(3+)} = Al^{3+}, Cr^{3+}, Fe^{3+}, Mn^{3+}$ , etc,  $A^{n-} = Cl^-, NO_3^-, ClO_4^-, CO_3^{2-}, SO_4^{2-}$  (Costa, 2007).

The behavior of LDHs is highly reactive to various organic anions, which can exchange as 80 - 100% of the interlayer anions in LDHs (Meyn et al., 1990). Moreover, it has high anion-exchange capacities and flexible interlayer space and can accommodate many materials such as contaminants from water, soil, sediment. Hence, it has been widely used as adsorbents, catalysts, catalyst supports and electronic chemical agents (Das et al., 2006)

There are several methods for the synthesis of LDHs such as the co-precipitation (Schouten et al., 2007; Reichle et al., 1986), the homogenous precipitation (Yang et al., 2004), the ion exchange (Khan and Hare, 2002) and hydrothermal crystallization method (Mascolo, 1995). However, all of methods may not be appropriate for every combination of metal ions. In this study, using the co-precipitation method synthesize the LDHs. The pH of the reaction is adjusted in a range of 8 -10 depending on the type of the metal ions. Then to obtain crystallized materials are suspended by hydrothermal treatment for a long period. It is an easy and efficient method to operation. However, the material is synthesized in powder form; it causes clogging during the use. Therefore, the granular form might be better form and studied.

## **2.4 Granular formation of adsorbent**

Techniques for the formation/fabrication of powder material which are mechanical coating and extrusion techniques are discussed herewith.

### **2.4.1 Mechanical coating technique**

The mechanical coating technique has been used in the formation of film on substrates of various materials with coating of metallurgy process in Figure 2.3. It was from the mixing powders in powder metallurgy process, in which metallic adhesions on the surfaces of alumina balls in a pot of a planetary ball mill occur because of mechanical friction and abrasion. Therefore, the mechanical coating is a simple and useful technique for forming film on round or spherical substrates (Yoshida et al., 2009). Other works presents the basis of mechanical that was a new ultrasonic-based dry mechanochemical method for coating metallic surface with other metal (e.g. Ti, SiC and Al<sub>2</sub>O<sub>3</sub>) or ceramic materials. This method had two modifications that were separated into two parts. The first part described that hard ball and metal or ceramic powder was put into a chamber which is fixed beneath the surface to be coated. Final part described that only balls were put into the chamber while the surface was precoated with a suspension of a liquid and powder. The chamber was set into high vibration by an ultrasonic transducer. The results showed that method allowed the various coatings and armored layers on the metallic surface production (Komarov et al., 2008).

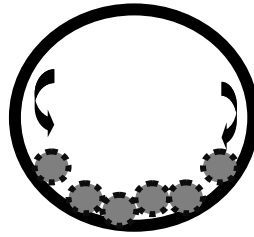


**Figure 2.3** Mechanical coating features.

### 2.4.2 Extrusion technique

In the extrusion process, the synthesis or modification of the polymeric material take place simultaneously with its processing and shaping at increased temperature into a product (Haba and Narkis, 2003), as shown in Figure 2.4.

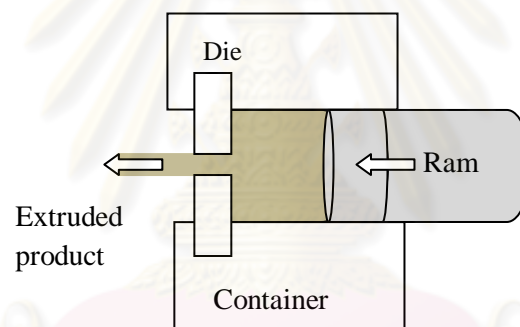


**Figure 2.4** Extrusion process.

This technique is inexpensive and provides good mixing and heat transfer at high viscosities, and may lead to improved compatibility. The polymeric materials were used widely such as polyethylene (PE) and polypropylene (PP) etc. that was a commercially available grade of low-density and high molecular weight. Costa (2007) investigated that preparing PE/LDHs based nano-composites in several parameter associated with the extruder quality of thermoplastics. The results showed that the suitable mixing of PE/LDHs in 1:1 weight ratio. Other works present the model was used for the description of extrusion pressure that using a paste containing zeolite, bentonite and water. It was found that this model was capable of predicting the extrusion pressure well (Li and Bridgwater, 2000). The main polymer used in this

study is polyacrylate as an aqueous emulsion copolymer of pure acrylic. This polymer was purchased the Chemical Village production, with trade name of ULTRABOND P261. Several benefits of this polymer are excellent weather durability, excellent water resistance and rubbing property and high gloss and good dispersing stability. The properties of the polymer are shown in Table 2.3.

**Table 2.3** Properties of the emulsion copolymer of pure acrylic

Appearance	Milky white liquid
Solid Content (%)	48-52
pH	7.5-9.5
Viscosity (Brookfield RVT)	< 500 (cps)
Particle Size	0.1-0.2
MFFT (°C)	20
Tg(°C)	20

ศูนย์วิทยทรัพยากร  
จุฬาลงกรณ์มหาวิทยาลัย

## CHAPTER III

### METHODOLOGY

The experiments consist of three steps including adsorbent synthesis, characterization of adsorbents, and phosphate adsorption experiments, which the details are described. The experiment approach is following the schematic diagram, presented in Figure 3.1. Chemicals and apparatus in this work are listed as follows;

#### 3.1 Chemicals and apparatus

##### 3.1.1 Chemicals

- Magnesium nitrate ( $\text{Mg}(\text{NO}_3)_2 \cdot 6\text{H}_2\text{O}$ ) (99%, Fluka)
- Aluminium nitrate ( $\text{Al}(\text{NO}_3)_3 \cdot 9\text{H}_2\text{O}$ ) (98%, Fluka)
- Ferric nitrate ( $\text{Fe}(\text{NO}_3)_3 \cdot 9\text{H}_2\text{O}$ ) (99%, Merck)
- Sodium carbonate ( $\text{Na}_2\text{CO}_3$ ) (99%, Univar)
- Sodium hydroxide ( $\text{NaOH}$ ) (99%, Merck)
- Dihydrogen orthophosphate ( $\text{KH}_2\text{PO}_4$ ) (99%, Univar)
- Ammonium molybdate ( $(\text{NH}_4)_6\text{Mo}_7\text{O}_{24} \cdot 4\text{H}_2\text{O}$ ) (81%, Chameleon)
- Ammonium metavanadate ( $\text{NH}_4\text{VO}_3$ ) (90%, Fluka)
- Activated carbon
- Hydrochloric acid ( $\text{HCl}$ ) (70%, Merck)
- Alumina granules ( $\varnothing$  0.5-1.2 mm)
- Acrylic emulsion (Chemical village Co., Ltd.)

##### 3.1.2 Apparatus

- Oven
- Magnetic stirrer
- pH meter
- Centrifuge
- Shaker

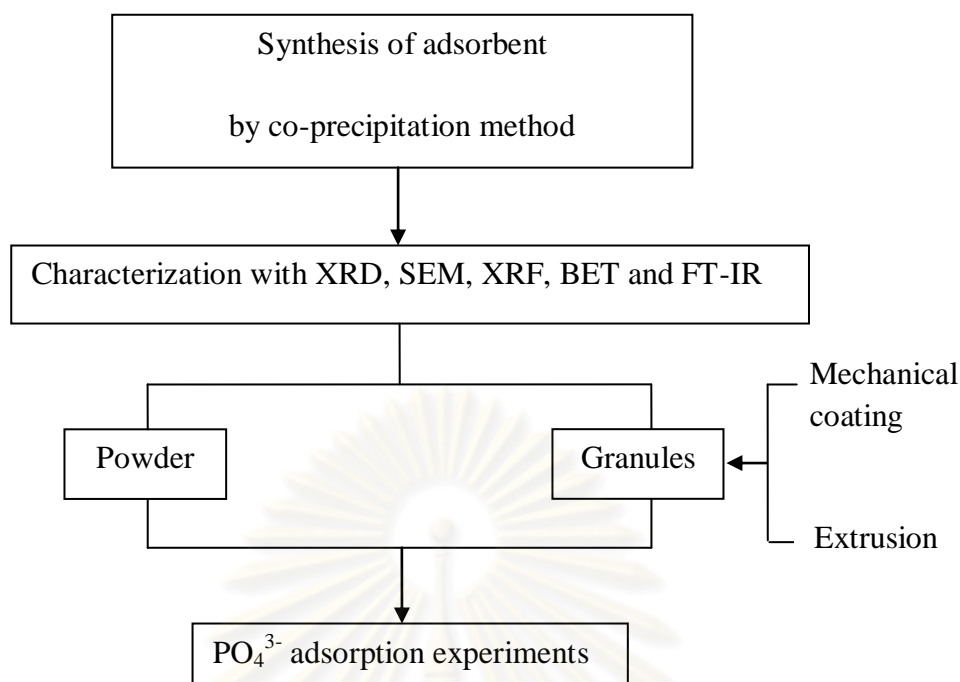


**Figure 3.1** Experimental scheme of this work.

## 3.2 Experimental procedures

### 3.2.1 Preparation of phosphate solution

A phosphate stock solution of 500 mg P/l was prepared by dissolving 2.1970 g of  $\text{KH}_2\text{PO}_4$  in one liter of deionized water. This phosphate solution was used as the synthesized wastewater. It was diluted by deionized water into different concentrations as 1, 5, 10, 20, 30 and 40 mg P/l. These are assigned as initial concentrations of adsorption experiments. The pH value of the phosphate solution was adjusted to 5.0 - 6.0 with diluted  $\text{HNO}_3$  and  $\text{NaOH}$  before adsorption experiments.

### 3.2.2 Material synthesis

$\text{Fe}_2\text{O}_3$ -Mg-Al and Mg-Al LDHs samples were synthesized by a co-precipitation method. The synthesis was modified from Das et al. (2006).

A mixed aqueous solution “A”, which contains 0.05 M  $\text{Mg}(\text{NO}_3)_2 \cdot 6\text{H}_2\text{O}$  (30 ml), 0.025 M  $\text{Al}(\text{NO}_3)_3 \cdot 9\text{H}_2\text{O}$  (30 ml) and 0.00125 M  $\text{Fe}(\text{NO}_3)_3 \cdot 9\text{H}_2\text{O}$  (30 ml) in 2: 1: 0.05 weight ratio for the  $\text{Fe}_2\text{O}_3$ -Mg-Al LDHs, and 0.05 M  $\text{Mg}(\text{NO}_3)_2 \cdot 6\text{H}_2\text{O}$  (45 ml) and 0.025 M  $\text{Al}(\text{NO}_3)_3 \cdot 9\text{H}_2\text{O}$  (45 ml) for the Mg-Al LDHs, was added to the water and stirred for 30 min. Simultaneously, a mixed aqueous solution “B” containing 0.5 M NaOH and 0.25 M  $\text{Na}_2\text{CO}_3$  was added to the water and stirred for 30 min. Then the solution B was added drop-wise to solution A. Afterwards, the pH of obtained solution was adjusted to be 10, and kept stirring continuously at room temperature for 24 h. afterwards, the suspension was aged at  $120^\circ\text{C}$  for 24 h and held for the crystallization. After aging, the precipitate was separated by centrifugation and washed with deionized water until pH of flushing rinse was of around 7. The obtained material was finally dried and calcined at  $550^\circ\text{C}$  for 6 h, as shown in Figure 3.2.

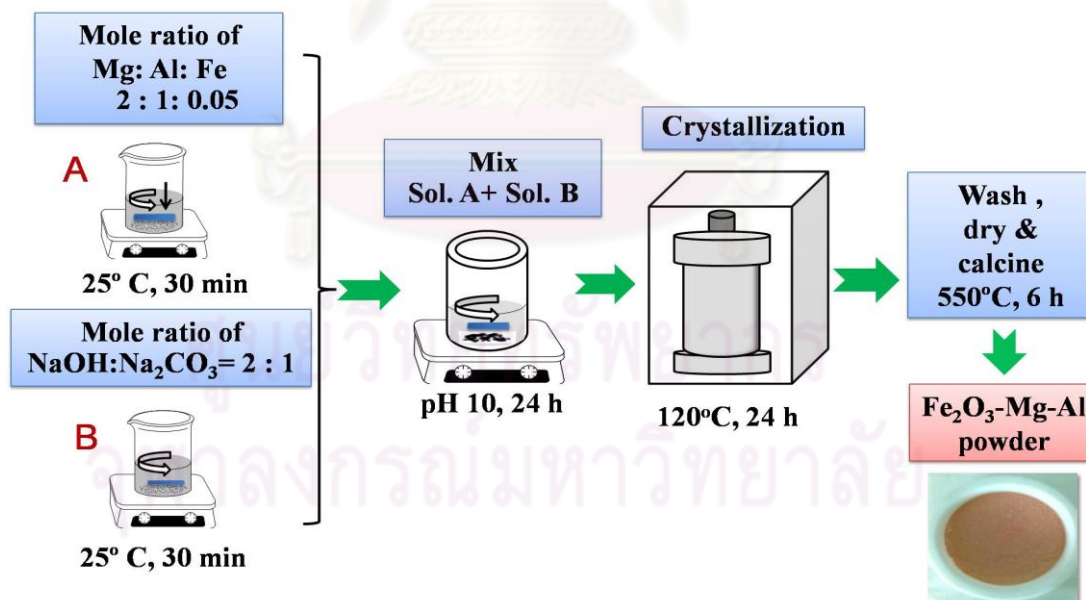


**Figure 3.2** Procedure of  $\text{Fe}_2\text{O}_3$ -Mg-Al LDHs synthesis.

### 3.3.3 Granular formation of sample

In this study, two granular formations are selected to study and described.

#### 3.3.3.1 Mechanical coating technique

The obtained  $\text{Fe}_2\text{O}_3\text{-Mg-Al}$  and  $\text{Mg-Al}$  LDHs powder were granulated by the mechanical coating technique. The synthesis was modified from Yoshida et al. (2009). Four grams of  $\text{Fe}_2\text{O}_3\text{-Mg-Al}$  powder and 6.00 g of alumina balls ( $\varnothing$  0.5-1.2 mm) in the case of  $\text{Fe}_2\text{O}_3\text{-Mg-Al}$  granules, and 4.00 g of  $\text{Mg-Al}$  powder for  $\text{Mg-Al}$  granules, were placed in a pot mill of 250 ml. Then a pot mill was rotated continuously with a rotation speed of 300 rpm for 24 h. After that the alumina balls with the  $\text{Fe}_2\text{O}_3\text{-Mg-Al}$  and  $\text{Mg-Al}$  film were separated from the remained powder. They were dried and calcined at  $550^\circ\text{C}$  for 24 h. The attached  $\text{Fe}_2\text{O}_3\text{-Mg-Al}$  and  $\text{Mg-Al}$  powder amount was calculated, as shown in Figure 3.3.



**Figure 3.3** Preparation of granules by mechanical coating.



### 3.3.3.2 Extrusion technique

The obtained  $\text{Fe}_2\text{O}_3$ -Mg-Al and Mg-Al LDHs powder were granulated by the extrusion technique. The synthesis was modified from Costa (2007). A mixed solution containing  $\text{Fe}_2\text{O}_3$ -Mg-Al LDHs and acrylic binder in several ratios (1:1, 1:0.5, 1:0.2, and 1:0.1 weight ratio) with a similar procedure, the solution of Mg-Al LDHs, was prepared to extrusion. Afterwards, the extruded strands of  $\text{Fe}_2\text{O}_3$ -Mg-Al and Mg-Al LDHs were granulated and dried at room temperature for 4 h, as shown in Figure 3.4.

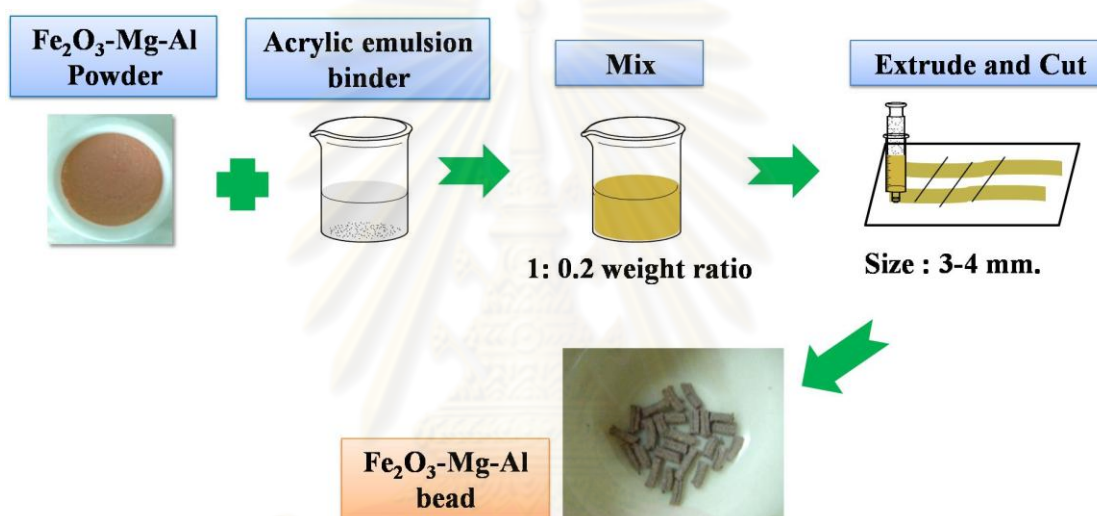


**Figure 3.4** Preparation of  $\text{Fe}_2\text{O}_3$  granules by extrusion.

ศูนย์วิทยทรัพยากร  
จุฬาลงกรณ์มหาวิทยาลัย

### 3.3.4 Adsorption studies

250 mg of each powdered sample was suspended in 250 ml phosphate solution containing various phosphate concentrations (1, 5, 10, 20, 30 and 40 mg P/l). The test was carried out at room temperature. The solution pH was adjusted to 5.0 - 6.0 with 0.5 M HNO<sub>3</sub> and 0.5 M NaOH. The suspensions were shaken at 115 rpm for 24 h. The contact times were 5, 10, 20, 30, 45, 60, 120, 240, 360, 540, 720, 900, 1080 and 1440 min. After complete the adsorption period about 24 h, the solution were filtered through 0.45 μm by membranes filter and analyzed the residue PO<sub>4</sub><sup>3-</sup> concentration following the spectrophotometrical vanadomolybdophosphoric acid method (APHA, 2005). The phosphate adsorption capacity was calculated from the decrease of the phosphate concentration in solutions and fitted to Langmuir and Freundlich isotherm equations. With a similar procedure, the effect of Fe<sub>2</sub>O<sub>3</sub>-Mg-Al LDHs and Mg-Al LDHs granules that followed by mechanical coating and extrusion techniques on phosphate adsorption was tested in a series of experiments using the same initial phosphate concentration (5 mg P/l) and a similar obtained pH, as shown in Figure 3.5.

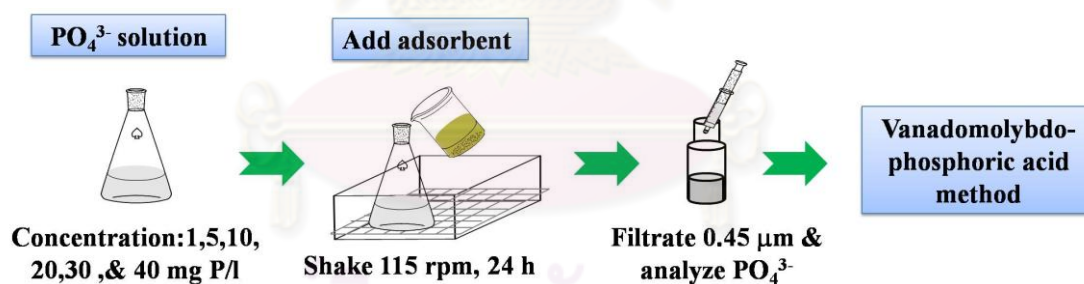


**Figure 3.5** Phosphate adsorption testing procedure.

### 3.4 Analytical methods

#### 3.4.1 Characterization

Powder Fe<sub>2</sub>O<sub>3</sub>-Mg-Al was characterized by X-ray diffraction (XRD), BET technique, Scanning Electron Microscopy (SEM). X-ray Fluorescence (XRF) and Fourier Transform Infrared (FT-IR).

XRD patterns were acquired with X-ray diffraction using CuK $\alpha$  radiation (40kV and 40 mA). XRD shows the detailed information of the chemical composition and crystalline structure of natural and manufactured materials. The major use of powder diffraction is to identify components in a sample by search/match procedure. All XRD patterns were obtained from 10° to 70° with a scan speed of 5.0°/min (Bruker axs D5005).

SEM use the areas ranging from about 1 cm. to 5  $\mu$ m in width that can be imaged in a scanning mode using conventional SEM technique (magnification in ranging from 20x to 30,000x, spatial resolution of 50 to 100 nm.) by JEOL JEM 2010.

The BET surface areas of the samples was determined following N<sub>2</sub> adsorption-desorption method at liquid nitrogen temperature (77K) by Quantasorb (Quantachrome, USA).

XRF was widely used to measure and identify the concentration of elemental composition of materials and were measured the mineral content of the extracted iron, which the dried samples are pressed at 30 N.m<sup>-2</sup> to make the pellet. The quantitative elemental was performed with the current of 100 mA and the potential of 24 kV (Philips PW 2004).

The IR spectra were recorded on a Perkin-Elmer 1725X spectrophotometer to check the change in the functional groups of the studied materials. It presents characteristic of the chemical bond that can be seen in the annotated spectrum. Molecular bond of the sample vibrates at various frequencies depending on the elements and the type of bonds.

### 3.4.2 Analysis

The vanadomolybdophosphoric acid method (APHA, 2005) was widely used to evaluate and confirms an unknown  $\text{PO}_4^{3-}$  concentration in solution. Prepared vanadate-molybdate reagent, which contained 2.5 g of  $(\text{NH}_4)_6\text{Mo}_7\text{O}_{24}\cdot 4\text{H}_2\text{O}$  in 30 ml of distilled water and 0.125 g of  $\text{NH}_4\text{VO}_3$  by heating to boiling point in 30 ml of distilled water. 33 ml of 0.5 N HCl was added when it cooled to dilute to 100 ml with the distilled water. The obtained solution was present yellow color.

In the phosphate concentration analysis, 3.0 ml of sample solution by pipettes was added 0.05 ml (1 drop) of phenolphthalein as indicator in a 25 ml beaker. Then 12 mg of activated carbon was added into the samples and shaken thoroughly for 5 min. Afterwards, the samples were filtrated to remove the carbon and 2.0 ml of sample was placed into 10 ml a sample bottle, which was added with 0.6 ml of vanadate-molybdate reagent and diluted to the mark with deionized water. After 10 min, the obtained samples were measured the absorbance at 470 nm by UV-Vis spectrophotometer. For blank reagents, using 2.5 ml of deionized water combine with vanadate-molybdate reagent as the reference solution. In addition, the preparation of a calibration curve from five standards within the  $\text{PO}_4^{3-}$  ranges was achieved, after that; absorbance was plotted with  $\text{PO}_4^{3-}$  concentration.

## CHAPTER IV

### RESULTS AND DISCUSSION

This chapter presents the results of this study which were separated into two parts. The first part presents characterization and adsorption studies of Fe<sub>2</sub>O<sub>3</sub>-Mg-Al LDHs and Mg-Al LDHs adsorbents in powder form. The characterizations include X-ray diffraction (XRD), Scanning electron microscopy (SEM), Fourier transform infrared (FT-IR), X-ray fluorescence (XRF) and Brunauer-Emmett-Teller technique (BET). The obtained adsorbents were studied for phosphate adsorption capacities. The adsorption isotherms including Langmuir and Freundlich isotherm are evaluated. In the second part, the same work was done in granular form of Fe<sub>2</sub>O<sub>3</sub>-Mg-Al LDHs and Mg-Al LDHs adsorbents.

#### 4.1 Powder form of adsorbents

Mg-Al LDHs and Fe<sub>2</sub>O<sub>3</sub>-Mg-Al LDHs were synthesized by co-precipitation technique. The following characterization results are used to confirm in their properties.

##### 4.1.1 Characterizations

Figure 4.1 shows the XRD patterns of Mg-Al LDHs and Fe<sub>2</sub>O<sub>3</sub>-Mg-Al LDHs compared to the standard LDHs (Das et al., 2006). For LDHs, a series of sharp peaks are observed. Both adsorbents have sharp diffraction peaks. The gallery spacing in the prepared samples of Mg-Al LDHs and Fe<sub>2</sub>O<sub>3</sub>-Mg-Al LDHs presented similar peaks to LDH platelets, especially related to the peak of (003) plane (characteristic peaks at  $2\theta = 11^\circ$ ). Other peaks at relatively high  $2\theta$  value are indexed to non-basal (006), (009), (110), and (113) reflections. However, it should be noted that the sharp character peak of LDHs become broad and with a low intensity in the composites. This suggests that a partial intercalation or exfoliation of the LDHs platelets might be taken place in the composites at  $11^\circ$ ,  $24^\circ$ , and  $35^\circ$  and broad, less intense peaks at  $38^\circ$ ,  $43^\circ$ ,  $48^\circ$ , and  $61^\circ$ . It was confirmed that the peak presented at the sample peak of a crystallized hydrotalcite-like phase (Mg-Al LDHs) (Kishore et al., 2008; Yang et al., 2003). After the incorporation of Fe<sub>2</sub>O<sub>3</sub> into the layers of LDHs, the peak at the  $2\theta$  of

11° and 48° decreased, while the peak at the 2θ of 43° increased because of the incorporated Fe<sub>2</sub>O<sub>3</sub> in LDHs structure (Chitrakar et al., 2007). Therefore, the intensity of the diffraction indicated that the LDH structure interacts with Fe<sub>2</sub>O<sub>3</sub>, was not destroyed and no shifting of their positions to lower 2θ values was explained as an increasing ion exchange capacity of the brucite-like layer, by adding Fe<sub>2</sub>O<sub>3</sub> or Fe<sup>3+</sup>.

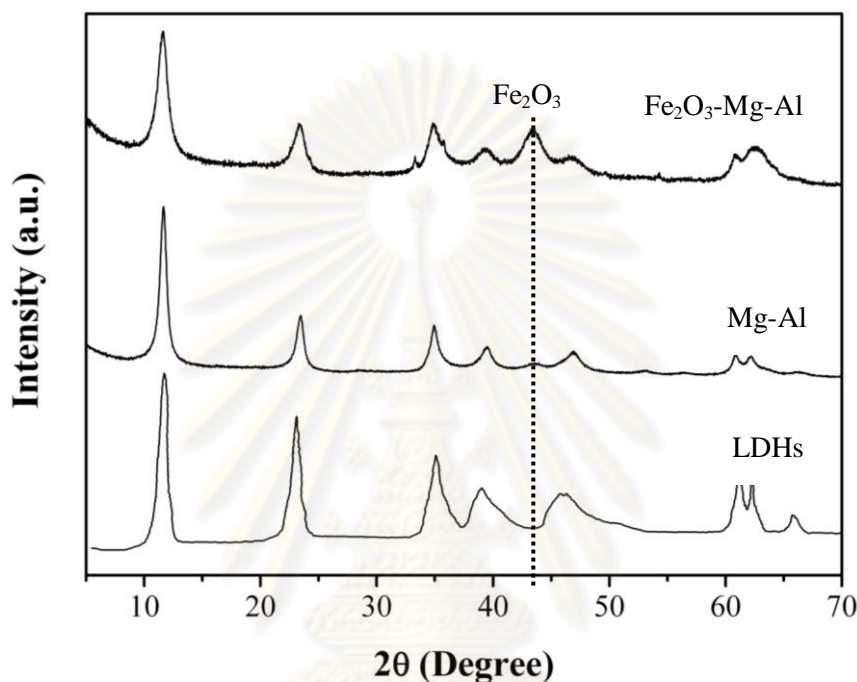


**Figure 4.1** XRD patterns of Fe<sub>2</sub>O<sub>3</sub>-Mg-Al LDHs, Mg-Al LDHs and LDHs (standard) (Das et al., 2006).

The SEM images of Fe<sub>2</sub>O<sub>3</sub>-Mg-Al LDHs and Mg-Al LDHs samples are presented in Figure 4.2. The image showed an aggregate of particles. As observed, the particle sizes are about less than 0.5 μm in both materials. Compared to the particle size released by Schouten et al. (2007), the prepared material was relatively smaller. The images of all samples have spherical shape, in spite of, incorporation of Fe<sub>2</sub>O<sub>3</sub> into LDHs structure. The figures indicated that LDHs structure combined with Fe<sub>2</sub>O<sub>3</sub>, did not affect to the original structure of Mg-Al LDHs and LDHs.

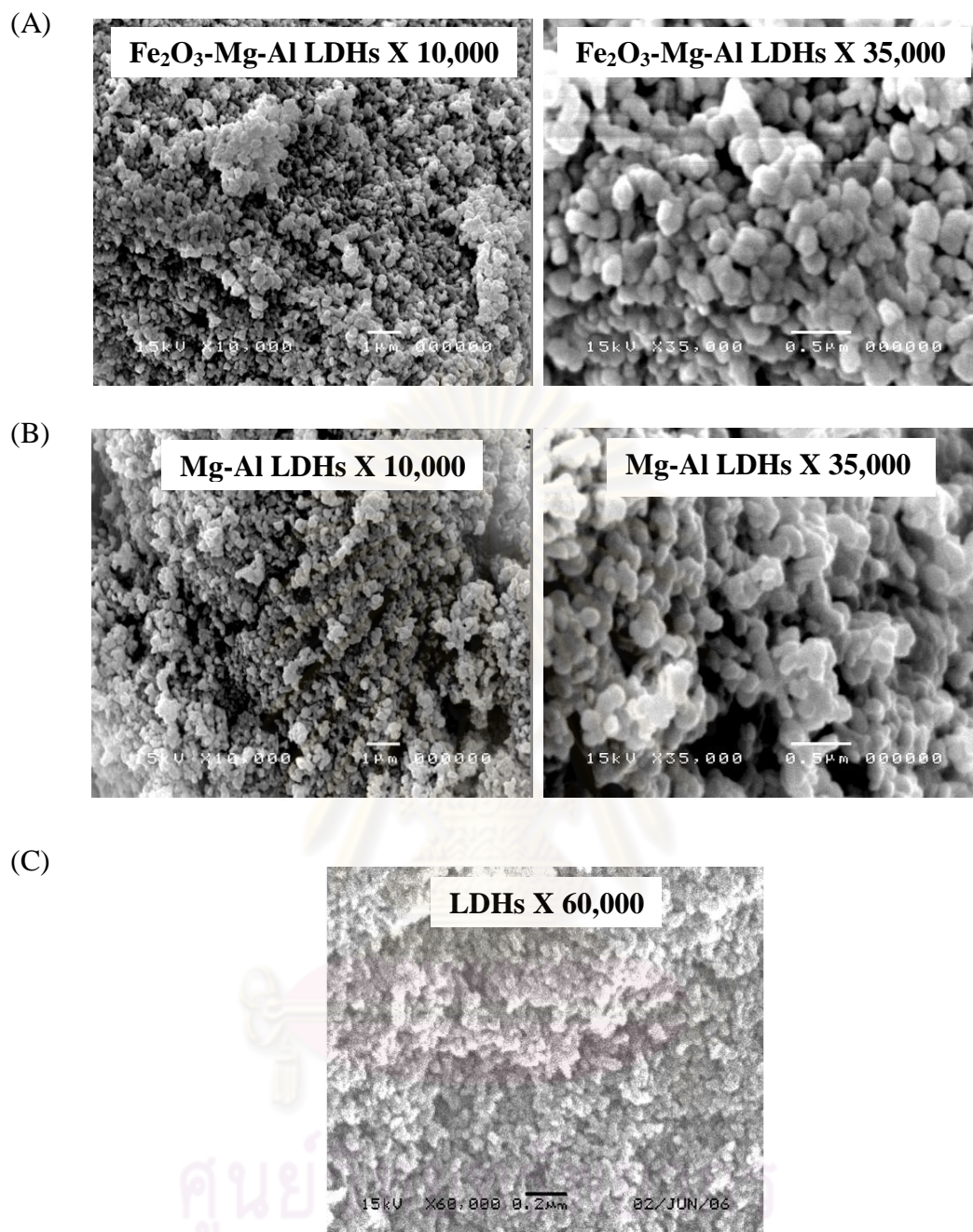


**Figure 4.2** SEM micrographs of (A) Fe<sub>2</sub>O<sub>3</sub>-Mg-Al LDHs, (B) Mg-Al LDHs and (C) LDHs (Schouten et al., 2007).

In order to ensure that  $\text{Fe}_2\text{O}_3$  was bonded into the samples as expected. FTIR of samples was analyzed. The spectrum of  $\text{Fe}_2\text{O}_3$ -Mg-Al and Mg-Al samples are shown in Figure 4.3. The spectrum of all LDH samples, exhibited Mg (Al)-O-Mg (Al) (at  $460\text{ cm}^{-1}$ ), Mg (Al)-O (at  $660\text{-}700\text{ cm}^{-1}$ ) and hydroxyl group ( $\text{OH}^-$ ) (at  $3450\text{ cm}^{-1}$ ) (Das et al., 2002; Yang et al., 2003; Geraud et al., 2006). In the spectrum of the  $\text{Fe}_2\text{O}_3$ -Mg-Al, the intensities of three bands of LDHs decreased while the intensities of Mg-Al bands increased because of incorporation of  $\text{Fe}_2\text{O}_3$  with LDH structure.

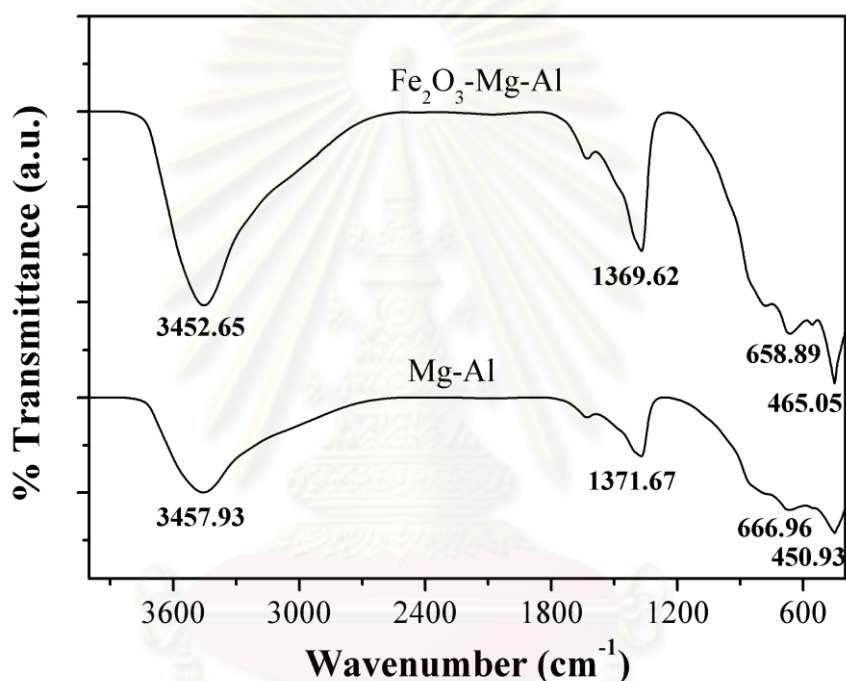


**Figure 4.3** FT-IR spectrum of  $\text{Fe}_2\text{O}_3$ -Mg-Al LDHs and Mg-Al LDHs.

The amounts of elements in all samples were examined by XRF as shown in Table 4.1. The main composition of  $\text{Fe}_2\text{O}_3$ -Mg-Al LDHs consisted of MgO,  $\text{Al}_2\text{O}_3$  and  $\text{Fe}_2\text{O}_3$ . Similarly, the main Mg-Al LDHs composition was MgO and  $\text{Al}_2\text{O}_3$ . Both adsorbents indicated that the ratio of synthesis contained 0.05:2:1 and 2:1 weight ratio for  $\text{Fe}_2\text{O}_3$ -Mg-Al LDHs and Mg-Al LDHs, respectively. This was to confirm that the ratio of synthesis. Moreover, the other compositions of samples included  $\text{SiO}_2$ ,  $\text{SO}_3$ , Cl and CaO, which they were not affect to the properties of prepared samples.



**Table 4.1** Chemical compositions of prepared materials

Sample	Amount of element (% of weight)			
	MgO	Al <sub>2</sub> O <sub>3</sub>	Fe <sub>2</sub> O <sub>3</sub>	Others
Fe <sub>2</sub> O <sub>3</sub> -Mg-Al LDHs	40.85	20.37	2.98	35.8
Mg-Al LDHs	42.50	21.39	-	36.11

The surface area is one of main factors for adsorption process. BET analysis was carried out and found that specific surface area of Fe<sub>2</sub>O<sub>3</sub>-Mg-Al LDHs and Mg-Al LDHs in powder form is 219.5 and 210 m<sup>2</sup>/g, respectively, as listed in the Table 4.2. In the comparison, the specific surface area of Mg-Al-Fe and Mg-Al studied by Vulic et al. (2008) was reported in Table 4.2. The obtained results were a bit lower than those from Vulic et al. (2008). Mg-Al-Fe and Mg-Al LDHs, which was synthesized with different ratio of Mg: Al: Fe. The higher concentration of M (III) ion was increased, resulting in the number of neighboring M (III) ions and the formation of additional M (III)-hydroxide phase. Therefore, a decrease of specific surface area in this study may be resulted from the appropriate concentration of M (III) ions.

**Table 4.2** BET surface areas of adsorbents

Adsorbent	BET area (m <sup>2</sup> /g)
Fe <sub>2</sub> O <sub>3</sub> -Mg-Al LDH	219.5
Mg-Al LDHs	210
Mg-Al-Fe <sup>a</sup>	270
Mg-Al <sup>a</sup>	230

<sup>a</sup> Vulic et al., 2008



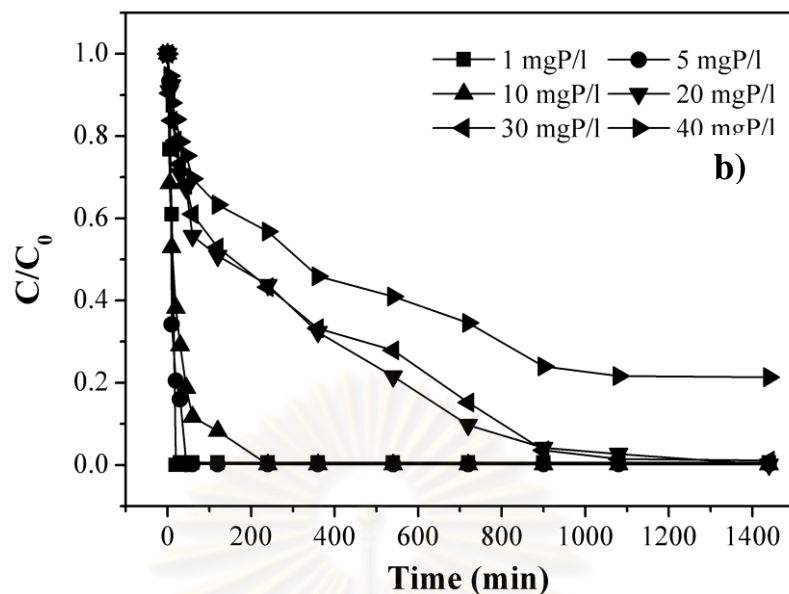


**Figure 4.4** Concentration profiles of remained phosphate in the solution over  
a)  $\text{Fe}_2\text{O}_3$ -Mg-Al LDHs and b) Mg-Al LDHs.

The experimental results could also provide the effect of initial concentration on phosphate adsorption by  $\text{Fe}_2\text{O}_3$ -Mg-Al LDHs and Mg-Al LDHs powder. The percentage of phosphate adsorption decreased with increased initial phosphate concentration from 99 % for 1 mg P/l to 78% for 40 mg P/l. This might be due to phosphate was run out in low concentration while the ability of LDHs still remained. Isotherm evaluation should be one key to explain this phenomena.

Since the removal of phosphate in low concentration (initial concentration of 1, 5 and 10 mg P/l) was completed, it is not able to be used to evaluate the adsorption isotherm (see in Figure 4.4). Thus those three concentrations were discarded due to no effect to calculate the adsorption isotherm. The rest data were plotted for adsorption on adsorbent mass basis, as shown in Figure 4.5. The investigation of equilibrium adsorptions, including Langmuir and Freundlich adsorption isotherms was carried out.

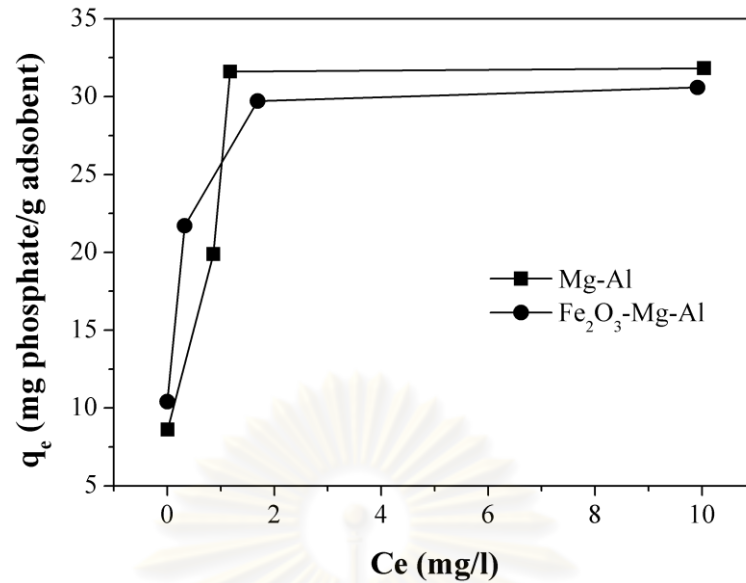


**Figure 4.5** Sorption of phosphate on Fe<sub>2</sub>O<sub>3</sub>-Mg-Al LDHs and Mg-Al LDHs at pH 5.5-5.7.

The calculations for the adsorption of phosphate on Fe<sub>2</sub>O<sub>3</sub>-Mg-Al LDHs and Mg-Al LDHs were linearly fitted to Langmuir and Freundlich models. The Langmuir isotherm was presented as express in equation 1.

$$q_e = \frac{bqC_e}{1 + qC_e} \quad (1)$$

and linearized to

$$\frac{C_e}{q_e} = \frac{1}{qb} + \frac{C_e}{q} \quad (2)$$

Where;

q<sub>e</sub> is the equilibrium phosphate concentration on the powder samples (mg/g)

C<sub>e</sub> is the equilibrium concentration of phosphate (mg/l)

q is the maximum sorption capacity (mg/g)

b is the Langmuir sorption constant (l/mg) that related to affinity of the binding sites (Boujelben et al., 2008)

In order to explain the applicability of phosphate adsorption equilibrium on  $\text{Fe}_2\text{O}_3$ -Mg-Al LDHs and Mg-Al LDHs, Freundlich adsorption isotherm was also applied. This is expressed by the following equation 3.

$$q_e = K_F C_e^{1/n} \quad (3)$$

and linearized to 
$$\log q_e = \log K_F + \frac{1}{n} \log C_e \quad (4)$$

Where;

$K_F$  is the Freundlich constant related to the adsorption capacity of the adsorbent

$n$  is a constant related to energy and intensity of adsorption (Boujelben et al., 2008)

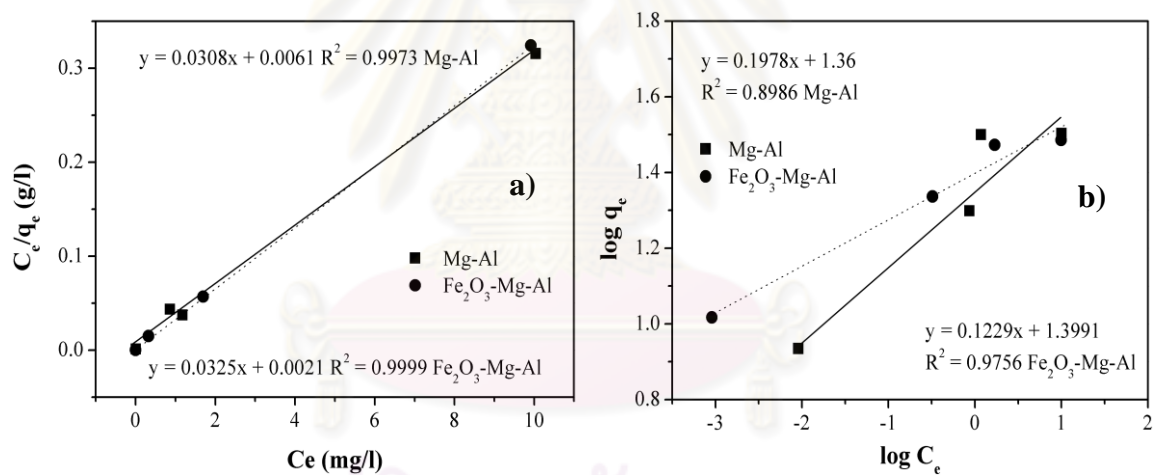


**Figure 4.6** Linearization of the plot; a) Langmuir isotherm and b) Freundlich isotherm.

Both isotherms were fitted based on the correlation coefficients ( $R^2$ ) in Figure 4.6. The value of  $b$  and  $q$  were determined from the slope and intercepts of the straight-line plots (Figure 4.6a) and were present in Table 4.3. It shows that  $R^2$  of Langmuir isotherm and Freundlich isotherm are 0.99 and 0.89 - 0.98, respectively. The value of  $b$  of  $\text{Fe}_2\text{O}_3$ -Mg-Al LDHs (16 L/mg) was higher than Mg-Al LDHs (5 L/mg) of two times because incorporation of  $\text{Fe}_2\text{O}_3$  in LDH structure may be effectively adsorbed phosphate concentration. In addition to the  $q$  values of both

Fe<sub>2</sub>O<sub>3</sub>-Mg-Al LDHs and Mg-Al LDHs was insignificantly different. The maximum value of q was around 30 - 33 mg/g of adsorbent.

Consider the Freundlich adsorption evaluation equation. The value of  $K_f$  and  $1/n$  obtained from the slope and intercepts of the straight-line plots in Figure 4.6(b). The value of  $K_f$  in Fe<sub>2</sub>O<sub>3</sub>-Mg-Al (25) was higher than Mg-Al (22). It indicates that the phosphate adsorption of Fe<sub>2</sub>O<sub>3</sub>-Mg-Al adsorbent was good. Accordingly to the value of  $1/n$ , all adsorbents had the value between 0 – 1 represent favorable phosphate adsorption on Fe<sub>2</sub>O<sub>3</sub>-Mg-Al LDHs and Mg-Al LDHs. The correlation coefficients ( $R^2$ ) for the Freundlich adsorption equation were less than Langmuir. As a result, Langmuir isotherm is better than fitted compared to Freundlich isotherm. Considering, the constant values for Langmuir isotherm.

**Table 4.3** Langmuir and Freundlich constants

Adsorbent	Langmuir			Freundlich		
	q (mg/g)	b (L/mg)	$R^2$	$K_F$	1/n	$R^2$
Fe <sub>2</sub> O <sub>3</sub> -Mg-Al	31.25	16.00	0.999	25.06	0.122	0.975
Mg-Al	33.33	5.00	0.997	22.91	0.197	0.898
Fe <sub>2</sub> O <sub>3</sub> tailings <sup>a</sup>	0.444	8.21	0.970	3.59	0.190	0.986

<sup>a</sup> The equation for phosphate (Zeng et al., 2004)

Further, the essential features of the Langmuir isotherm can be described by separation factor,  $R_L$  which is defined by the following equation (Hall et al., 1966):

$$R_L = \frac{1}{1 + bC_0} \quad (5)$$

Where;

$C_0$  is optimum initial concentration of phosphate (mg P/l)

b is Langmuir constant (l/mg)

The values of  $R_L$  indicate the nature of the adsorption process as given:  $R_L > 1$ ; for unfavorable,  $R_L = 1$ ; for linear,  $0 < R_L < 1$ ; for favorable and  $R_L = 0$ ; for irreversible. In the present study, the values of  $R_L$  with initial phosphate concentration. The results shows that the  $R_L$  values of  $\text{Fe}_2\text{O}_3$ -Mg-Al LDHs and Mg-Al LDHs were in the range of zero to one which indicates that the adsorption process is favorable for both adsorbents. The  $R_L$  values of  $\text{Fe}_2\text{O}_3$ -Mg-Al LDHs had higher than these values of Mg-Al LDHs at low concentration condition.

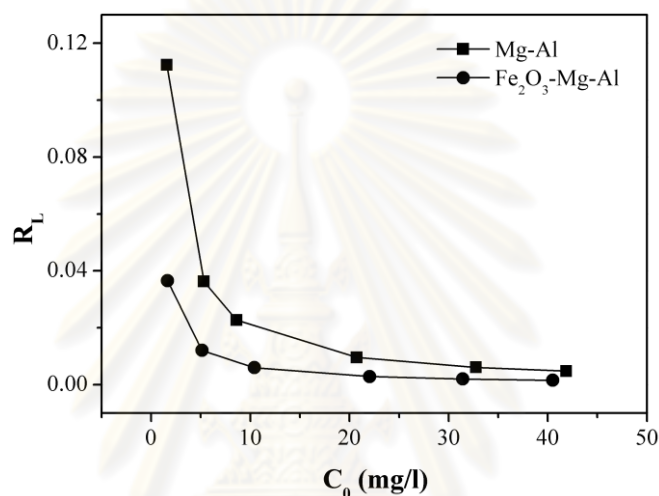


**Figure 4.7** Separation factor ( $R_L$ ) as a function of initial phosphate concentration.

In summary, the phosphate adsorption capacity on  $\text{Fe}_2\text{O}_3$ -Mg-Al LDHs and Mg-Al LDHs in powder form indicated that both  $\text{Fe}_2\text{O}_3$ -Mg-Al LDHs and Mg-Al LDHs had the obtained equilibrium time about 1440 min. In addition, studying the effect of initial phosphate concentration showed that the percentage of adsorption of both adsorbents decreased with increased initial phosphate concentration. The adsorption isotherms were fitted well to a linearized of Langmuir isotherm equation that described all adsorbate formed monolayer coverage on homogenous surface.

### 4.1.3 Kinetic study

The adsorption kinetic study was to estimate how well the behavior of adsorption before reaching equilibrium. The adsorption rate can be determined by using kinetic model, which calculated by the change of phosphate concentration over the time. The kinetic equation based on the adsorption capacities, as Lagergren's first-order rate equation. It is summarized as follows:

$$\frac{dq_t}{dt} = k_1(q_e - q_t) \quad (6)$$

and it is integrated with the boundary conditions of  $t = 0$  to  $t = t$  and  $q = q_t$  to yield

$$\log(q_e - q_t) = \log q_e - \frac{k_1}{2.303}t \quad (7)$$

Where;

$q_e$  is the adsorption capacities at equilibrium (mg/g)

$q_t$  is the adsorption capacities at any time,  $t$  (mg/g)

$k_1$  is the rate constant of the first-order adsorption ( $\text{min}^{-1}$ )

In order to describe chemisorptions involving covalent forces that to share the electrons between the adsorbent and adsorbate (Ho, 2006b). The kinetic rate equations can be rewritten as follows:

$$\frac{dq_t}{dt} = k_2(q_e - q_t)^2 \quad (8)$$

After integrating, this equation has a linear form of

$$\frac{t}{q_t} = \frac{1}{k_2 q_e^2} + \frac{1}{q_e}t \quad (9)$$

Where;

$q_e$  is the adsorption capacities at equilibrium (mg/g)

$q_t$  is the adsorption capacities at any time,  $t$  (mg/g)

$k_2$  is the rate constant of adsorption (mg/g min)



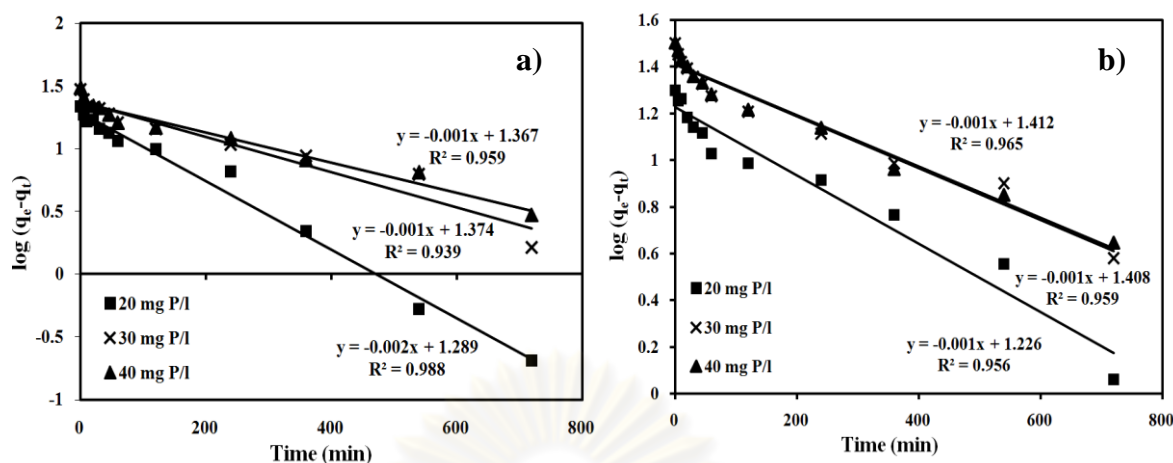


**Figure 4.8** Linear plots of pseudo-first-order model for phosphate adsorption on a)  $\text{Fe}_2\text{O}_3\text{-Mg-Al LDHs}$  and b)  $\text{Mg-Al LDHs}$ .

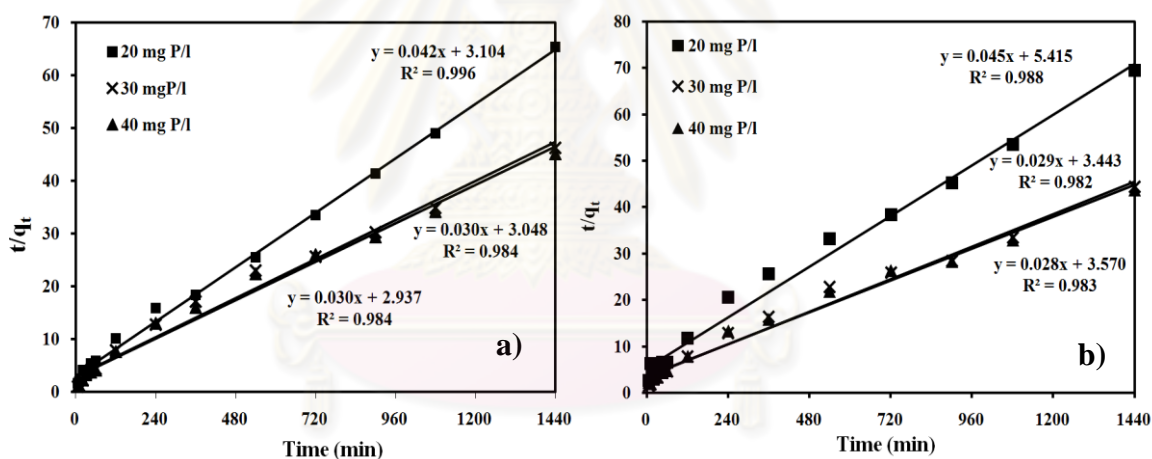


**Figure 4.9** Linear plots of pseudo-second-order model for phosphate adsorption on a)  $\text{Fe}_2\text{O}_3\text{-Mg-Al LDHs}$  and b)  $\text{Mg-Al LDHs}$ .

Both the adsorption kinetic models of pseudo-first-order were fitted based on the correlation coefficients ( $R^2$ ) in Figure 4.8. The rate constant ( $k$ ) and the equilibrium adsorption capacity ( $q_e$ ) can be determined from the slope and intercept of the straight-line plots (Figure 4.8) and were present in Table 4.4. It shows that  $R^2$  of pseudo-first-order model on  $\text{Fe}_2\text{O}_3\text{-Mg-Al LDHs}$  and  $\text{Mg-Al LDHs}$  are 0.93 - 0.98 and 0.95 - 0.96, respectively. The values of  $q_e$  of  $\text{Fe}_2\text{O}_3\text{-Mg-Al LDHs}$  were different insignificantly with  $\text{Mg-Al LDHs}$ . The comparison between adsorption capacities

from the experiment and kinetic model on both adsorbents showed that the adsorption capacity from pseudo-first-order models (16 - 25 mg/g) was badly with the adsorption capacity values from experiment (30 - 33 mg/g). For the  $k$  values of both  $\text{Fe}_2\text{O}_3$ -Mg-Al LDHs and Mg-Al LDHs were different insignificantly.

The pseudo-second-order models on both adsorbents were fitted based on the correlation coefficients ( $R^2$ ) in Figure 4.9. It shows that  $R^2$  of pseudo-first-order model on  $\text{Fe}_2\text{O}_3$ -Mg-Al LDHs and Mg-Al LDHs are 0.98 - 0.99 and 0.98, respectively. The rate constant ( $k$ ) and the equilibrium adsorption capacity ( $q_e$ ) obtained from the slope and intercept of the straight-line plots (Figure 4.9) and were present in Table 4.4. The  $q_e$  values of  $\text{Fe}_2\text{O}_3$ -Mg-Al LDHs (24 - 33 mg/g) were different insignificantly with Mg-Al LDHs (22 - 35 mg/g). They were found that the pseudo-second-order models almost agreed with the experimental adsorption capacity (30 - 33 mg/g). For the values of  $k$  of  $\text{Fe}_2\text{O}_3$ -Mg-Al LDHs ( $6 \times 10^{-4}$  -  $3 \times 10^{-4}$  mg/g min) and Mg-Al LDHs ( $3 \times 10^{-4}$  -  $2 \times 10^{-4}$  mg/g min) were different significantly. These confirmed that the phosphate adsorption on both adsorbents was fitted well with the pseudo-second-order kinetic model.  $\text{Fe}_2\text{O}_3$ -Mg-Al LDHs present the high adsorption capacity with short equilibrium time.

Accordingly, the pseudo-second-order kinetic model showed that the adsorption mechanism is predominant and the rates of phosphate adsorption process appear to control by the chemical adsorption (Chiou and Li, 2003). This adsorption mechanism may involve covalent force through the sharing of electrons between phosphate and adsorbents (Chen et al., 2008).

ศูนย์วิทยทรัพยากร  
จุฬาลงกรณ์มหาวิทยาลัย

**Table.4.4** Pseudo-first-order and pseudo-second-order kinetic constants and correlation coefficient ( $R^2$ ) for adsorption phosphate on  $Fe_2O_3$ -Mg-Al LDHs and Mg-Al LDHs adsorbents

Adsorbent	Initial $PO_4^{3-}$ conc. (mg P/l)	Pseudo-first-order			Pseudo-second-order		
		$q_e$ (mg/g)	$k_1 \times 10^{-3}$ ( $min^{-1}$ )	$R^2$	$q_e$ (mg/g)	$k_2 \times 10^{-4}$ (mg/g min)	$R^2$
$Fe_2O_3$ -	20	19.45	-4.60	0.99	23.81	5.680	0.99
Mg-Al	30	23.66	-2.30	0.94	33.33	2.946	0.98
	40	23.28	-2.30	0.96	33.33	3.060	0.98
Mg-Al	20	16.83	-2.30	0.96	22.22	3.741	0.99
	30	25.59	-2.30	0.96	34.48	2.441	0.98
	40	25.82	-2.30	0.97	35.71	2.200	0.98

## 4.2 Granular form of adsorbents

The obtained  $Fe_2O_3$ -Mg-Al LDHs and Mg-Al LDHs powder in the first parts were applied to form granular adsorbents for the use. The granules would decrease the clogging problem in the unit operation and the difficulty of adsorbents reuse. Mechanical coating and extrusion technique were two methods to be done. The physical properties and the adsorption compared to powder form were discussed.

### 4.2.1 Surface area

The specific surface area of granular formation of  $Fe_2O_3$ -Mg-Al LDHs and Mg-Al LDHs with mechanical coating and extrusion methods was 185.4, 201.6, 0.942 and 1.043  $m^2/g$ , respectively as tabulated in Table 4.5. The result showed that the specific surface areas of the both granular adsorbents of mechanical coating were higher than extrusion method. Some results were observed by Boujelben et al. (2008). The specific surface area of mechanical coating was less than that of alumina ball. This would be due to the materials of LDH compounds clog the mesopores and/or macropores of alumina balls.

**Table 4.5** BET surface areas of granular adsorbents

<b>Adsorbent</b>	<b>BET area (m<sup>2</sup>/g)</b>
Fe <sub>2</sub> O <sub>3</sub> -Mg-Al LDHs by mechanical coating	185.4
Mg-Al LDHs by mechanical coating	201.6
Alumina ball	340.0
Fe <sub>2</sub> O <sub>3</sub> -Mg-Al LDHs by extrusion	0.942
Mg-Al LDHs by extrusion	1.043
Fe <sub>2</sub> O <sub>3</sub> coated sand <sup>a</sup>	2.609

<sup>a</sup> Boujelben et al., 2008

### 4.2.2 Phosphate adsorption

The experiment was studied the percentage of adsorption of phosphate on the Fe<sub>2</sub>O<sub>3</sub>-Mg-Al LDHs and Mg-Al LDHs granular of mechanical coating and extrusion with acrylic emulsion binder techniques. This effect of both samples on the initial concentration of phosphate 5 mg P/l, at pH 5.5 and ambient temperature was studied at the same amount of adsorbent powder (1 g/l). The results are shown in Figure 4.8. The percentage of phosphate adsorption on granulated Fe<sub>2</sub>O<sub>3</sub>-Mg-Al LDHs (99%) was higher than that on Mg-Al LDHs (90%). However, the comparison of percent adsorption between alumina balls and Fe<sub>2</sub>O<sub>3</sub>-Mg-Al LDHs granular was similar because amount of phosphate might be depleted at this concentration level. The higher concentration condition of phosphate might be shown different results.

The case of the extrusion technique, the results were shown in Figure 4.8. The percentage of phosphate adsorption of granulated Mg-Al LDHs (76.63 %) was about 6% higher than Fe<sub>2</sub>O<sub>3</sub>-Mg-Al LDHs (70.29 %). According to the property of acrylic emulsion binder, it might result the agglomeration surface area of adsorbent. It related to the low specific surface area observed with iron oxide coated sand (2.609 m<sup>2</sup>/g) by Boujelben et al. (2008).

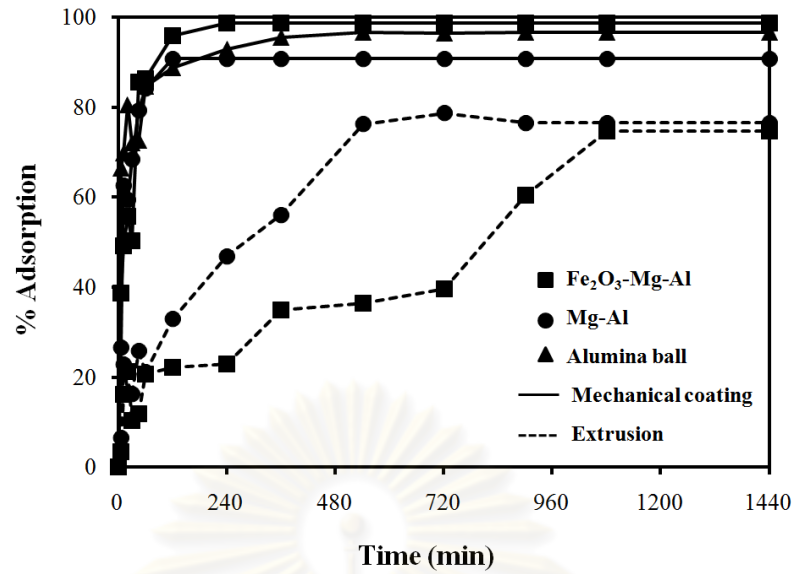


**Figure 4.10** Percentage of phosphate adsorption on granulated Fe<sub>2</sub>O<sub>3</sub>-Mg-Al LDHs and Mg-Al LDHs by mechanical coating and extrusion techniques.

## CHAPTER V

### CONCLUSION AND RECOMMENDATIONS

#### 5.1 Conclusion

$\text{Fe}_2\text{O}_3$ -Mg-Al and Mg-Al were synthesized by a co-precipitation method. The material was in layered double hydroxides (LDHs) form, confirmed by XRD, SEM, XRF, FT-IR and BET specific surface area. There was no collapsing of the LDHs structure after the insertion of  $\text{Fe}_2\text{O}_3$ . In addition, the addition of  $\text{Fe}_2\text{O}_3$  to the structure increased the specific surface area and affect to the adsorption capacity for phosphate.

The phosphate adsorption on  $\text{Fe}_2\text{O}_3$ -Mg-Al LDHs in powder form was 31 mg P/g  $\text{Fe}_2\text{O}_3$ -Mg-Al LDHs and higher than another adsorbent (Mg-Al LDHs), because of an incorporation of  $\text{Fe}_2\text{O}_3$  in LDH structure. The equilibrium time was reached in the adsorption system of these adsorbents longer than 1,000 min. To study the effect of initial phosphate concentration showed that the percentage of adsorption of both adsorbents decreased with increased initial phosphate concentration. Under equilibrium adsorption, the adsorption isotherms of both Mg-Al LDHs and  $\text{Fe}_2\text{O}_3$ -Mg-Al LDHs for phosphate adsorption were fitted well to the Langmuir isotherm describing monolayer coverage on homogenous surface.

The adsorption rate of phosphate adsorption on both adsorbents could be well described by the pseudo-second-order model as evidenced from the agreement between the experimental and kinetic model values.

The granular formation of both adsorbents with mechanical coating technique had higher the percentage of phosphate adsorption than that of extrusion technique. This might be noted that high surface areas of granular adsorbent by mechanical coating could adsorb to phosphate concentration.

## 5.2 Recommendations

1. Only one species in synthesized waste water was studied, the real waste water should be studied for unexpected stimulus; for examples anions such as sulfate ion, nitrate ion and carbonate ion.

2. The study of spent adsorbents for being fertilizer should be carried out. The effect of its use should be addressed.

3. The loading of adsorbents might be too high (1 g/l) for studying the adsorption equilibrium of phosphate at low initial concentration (1-10 mg P/l) so the loading of  $\text{Fe}_2\text{O}_3$ -Mg-Al LDHs and Mg-Al LDHs adsorbents should be done with the loading less than 1 g/l.



## REFERENCES

- Akay, G., Keskinler, B., Cakici, A., and Danis, U. Phosphate removal from water by red mud cross flow microfiltration. Water Research 32 (1998): 717-726.
- Akewaranugulsiri, S. Adsorption behavior of Cu<sup>2+</sup> from aqueous solution on composite crosslinked chitosan-clay. Master's Thesis, Department of Science Program in Environmental Management Faculty of Graduate School Chulalongkorn University. (2008).
- APHA/AWWA/WEF. Standard Methods for the Examination of Water and Wastewater [Online]. American Public Health Association/American Water Works Association/Water Environment Federation, Washington, DC, 1999. Available from: <http://apha.org/Book and Other media/pdf> [2011, January 20].
- Boujelben, N., Bouzid, J., Elouear, Z., Feki, M., Jamoussi, F., and Montiel, A. Phosphorus removal from aqueous solution using iron coated natural and engineered sorbents. Journal of Hazardous Matter 151 (2008): 103-110.
- Brunaues, P.H. Emmett and Teller, E. Adsorption of gases in multimolecular layers. Journal of American Chemical Society 60 (1935): 309-319.
- Cavani, F., Trifiro, F., and Vaccari, A. Hydrotalcite-type anionic clays: Preparation, properties and applications. Catalysis Today 11(1991): 173-301.
- Chang, M.Y., and Juang, R.S. Adsorption of tannia acid, humic acid and dye from water using the composite of chitosan and activated clay. Journal of Colloid Interface Science 278 (2004): 18-25.
- Chang, R. Chemistry. 9<sup>th</sup> edition. New York: McGraw-Hill Science/Engineer/Math. (2006).
- Chen, J., Kong, H., Wu, D., Hu, Z., Wang, Z., and Wang Y. Removal of phosphate from aqueous solution by zeolite synthesized from fly ash. Journal of Colloid Interface Science 300 (2006): 491-497.



- Chen, A.H., Liu, S.C., and Chen, C.Y. Comparative adsorption of Cu(II), Zn(II), and Pb(II) ions in aqueous solution on the crosslinked chitosan with epichlorohydrin. Journal of Hazardous Matter 514 (2008): 184-191.
- Chiou, M.S., and Li, H.Y. Adsorption behavior of reactive dye in aqueous solution on chemical cross-linked chitosan beads. Chemosphere 50 (2003): 1095-1105.
- Chitrakar, R., Tezuka, S., Sonoda, A., Sakane, K., and Hirotsu, T. Selective adsorption of phosphate from seawater and wastewater by amorphous zirconium hydroxide. Journal of Colloid and Interface Science 297(2006): 426-433.
- Cosimo, I.J., Diez, K.V., Xu, M., Iglesia, E., and Apesteguia, R.C. Structure and surface and catalytic properties of Mg-Al basic oxides. Journal of Catalysis 178 (1998): 492-510.
- Costa, F.R. Mg-Al Layered Double Hydroxide: A Potential Nanofilter and Flame-Retardant for Polyethylene. Doctor's Thesis, Faculty of Mechanical Engineering Technische University Germany. (2007).
- Cussler, E.L. Diffusion: Mass Transfer in Fluid Systems, 2<sup>nd</sup> edition. P.308-330. (1997).
- Das, J., Patra, B.S., Baliarsingh, N., and Parida, K.M. Adsorption of phosphate by layered double hydroxides in aqueous solutions. Applied Clay Science 32 (2006): 252-260.
- De-Bashan, L.E., and Bashan, Y. Recent advances in removing phosphorus from wastewater and its future use as fertilizer. Water Research 38 (2004): 4222-4246.
- Egerton, R.F. Physical principle of electron microscopy: an introduction to TEM, SEM, AEM. Springer 202 (2005).
- Faust, S.D., and Aly, O.M. Chemistry of Water Treatment. 2<sup>nd</sup> edition. Florida: CRC Press LLC, (1998).

- Genz, A., Kornmuller, A., and Jekel, M. Advanced phosphorus removal from membrane filtrates by adsorption on activated aluminium oxide and granulated ferric hydroxide. Water Research 38 (2004): 3523-3530.
- Grisdanurak, N., and Wittayakun, J. Catalyst: Fundamental and Application. 1<sup>st</sup> edition. Thammasat University. (2004).
- Haba, Y. and Narkis, M. Development and characterization of reactive extruded PVC/polyacrylate blends. Polymers of Advanced Technologies 16 (2005): 495-504.
- Ho, Y.S. Review of second-order models for adsorption systems. Journal of Hazard Matter B136 (2006a): 681-689.
- Ho, Y.S. Second-order kinetic model for sorption of cadmium onto tree fern: A comparison of linear and non-linear methods. Water Research. 40 (2006b): 119-125.
- Khan, A.I. and Hare, D.O. Intercalation chemistry of layered double hydroxides: recent developments and applications. Journal of Materials Chemistry 12 (2002): 3191-3198.
- Kishore, D. and Rodrigues, E.A. Liquid phase catalytic oxidation of isophorone with tert-butylhydroperoxide over Cu/Co/Fe-MgAl ternary hydrotalcites. Applied Catalysis 345 (2008): 104-111.
- Kuzawa, K., Jung, J.Y., Kiso, Y., Yamada, T., Nagai, M., and Lee, G.T. Phosphate removal and recovery with a synthetic hydrotalcite as an adsorbent. Chemosphere 62 (2006): 45-52.
- Manju, G.N., and Anirudhan, T.S. Evaluation of coconut carbon for the removal of arsenic from water. Water Research 32 (1998): 3062-3070.
- Mascolo, G. Synthesis of anionic clays by hydrothermal crystallization of amorphous precursors. Applied Clay Science 10 (1995): 21-30.
- Meyn, M., Beneke, K. and Legaly, G. Anionic-exchange reactions of layered double hydroxides. Inorganic Chemistry 29 (1990): 5201-5207.

- Miyauchi, H., and others. Phosphate adsorption site on zirconium ion modified Mg-Al layered double hydroxides. Topics in Catalysis 52 (2009): 714-723.
- Namasivayam, C. and Prathap, K. Recycling Fe(III)/ Cr(III) hydroxide, an industrial solid waste for the removal of phosphate from water. Journal of Hazardous Matter 123 (2005): 127-134.
- Neufeld, R.D. and Thodos, G. Removal of orthophosphate from aqueous solutions with activated alumina. Chemical Engineering Department 3 (1969): 661-667.
- Ozacar, M. Equilibrium and kinetic modeling of adsorption of phosphate on calcined alunite. Adsorption 9 (2003): 125-132.
- Reichle, W.T. Synthesis of anionic clay minerals (mixed metal hydroxides, hydrotalcite). Solid State Ionics 22 (1986): 135-141.
- Schouten, N., G.J.W., Euverink, W., and De Haan, B.A. Optimization of layered double hydroxide stability and adsorption capacity for anionic surfactants. Adsorption 13 (2007): 523-532.
- United States Environmental Protection Agency. Phosphorus: Water Quality Standards Criteria Summaries: A Compilation of State/Federal Criteria [Online]. National Service Center for Environmental Publications (NSCEP), 1988. Available from: <http://nepis.epa.gov/Exe/ZyNET.exe> [2011, January 30].
- Vulic, T., Hadnadjev, M., and Marinkovic-Neducin, R. Structure and morphology of Mg-Al-Fe mixed oxides derived from layered double hydroxides. Journal of Microscopy 232 (2008): 634-638.
- Wang, C.Y., Zhai, J.P., Nie, R., and Huang, L. Experimental study on phosphorus removal by activated sludge process in treating wastewater of low phosphorus concentration. Environmental Protection Science 31 (2005): 4-6.
- Xu, X., Gao, B., Wang, W., Yue, Q., Wang, Y., and Ni, S. Adsorption of phosphate from aqueous solution onto modified whet residue: characteristic, kinetic, column studies. Colloids and Surfaces B: Biointerface 70 (2009): 46-52.

- Yang, P., Yu, J., Wang, Z., Liu, Q., and Wu, T. Urea method for the synthesis of hydrotalcite reaction. Kinetic Catalyst Letter 83 (2004): 275-282.
- Yang, Z.Q., Zhang, G.C., Sun, J.D., and Jin, L.Z. Studies on synthesis and properties of Mg-Al-nitrate layered double hydroxides. Chinese Chemical Letters 14 (2003): 79-82.
- Ye, H., Chen, F., Sheng, Y., Sheng, G., and Fu, J. Adsorption of phosphate from aqueous solution onto modified palygorskites. Separation and Purification Technology 50 (2006): 283-290.
- Yildiz, E. Phosphate removal from water by fly ash using crossflow microfiltration. Separation and Purification Technology 35 (2004): 241-252.
- Yoshida, H. Lu, H. Nakayama, H., and Hirohashi, M. Fabrication of TiO<sub>2</sub> film by mechanical coating technique and its photocatalytic activity. Journal of Alloy and Compounds 475 (2009): 383-386.
- You, Y., Vance, F.V., and Zhao, H. Selenium adsorption on Mg-Al and Zn-Al layered double hydroxides. Applied Clay Science 20 (2001): 13-25.
- Zeng, L., Li, X., and Liu, J. Adsorptive removal of phosphate from aqueous solutions using iron oxide tailings. Water Research 38 (2004): 1318-1326.



APPENDIX

ศูนย์วิทยทรัพยากร  
จุฬาลงกรณ์มหาวิทยาลัย

**Table 1**  $C/C_0$  of phosphate using  $\text{Fe}_2\text{O}_3\text{-Mg-Al}$  LDHs in powder form as adsorption in terms of time and initial phosphate concentration

Time (min)	$C/C_0$					
	1 mg P/l	5 mg P/l	10 mg P/l	20 mg P/l	30 mg P/l	40 mg P/l
0	1	1	1	1	1	1
5	0.710	0.560	0.455	0.866	0.835	0.872
10	0.564	0.36	0.412	0.764	0.740	0.799
20	0.0005	0.308	0.208	0.783	0.728	0.789
30	0.0005	0.285	0.175	0.667	0.719	0.77
45	0.0005	0.200	0.145	0.623	0.65	0.708
60	0.0005	0.1408	0.105	0.534	0.56	0.64
120	0.0005	0.0001	0.058	0.461	0.51	0.61
240	0.0005	0.0001	8.73E-05	0.312	0.39	0.543
360	0.0005	0.0001	8.73E-05	0.114	0.333	0.445
540	0.0005	0.0001	8.73E-05	0.038	0.25	0.405
720	0.0005	0.0001	8.73E-05	0.023	0.106	0.317
900	0.0005	0.0001	8.73E-05	0.014	0.053	0.244
1080	0.0005	0.0001	8.73E-05	4.13E-05	0.013	0.219
1440	0.0005	0.0001	8.73E-05	4.13E-05	0.009	0.212

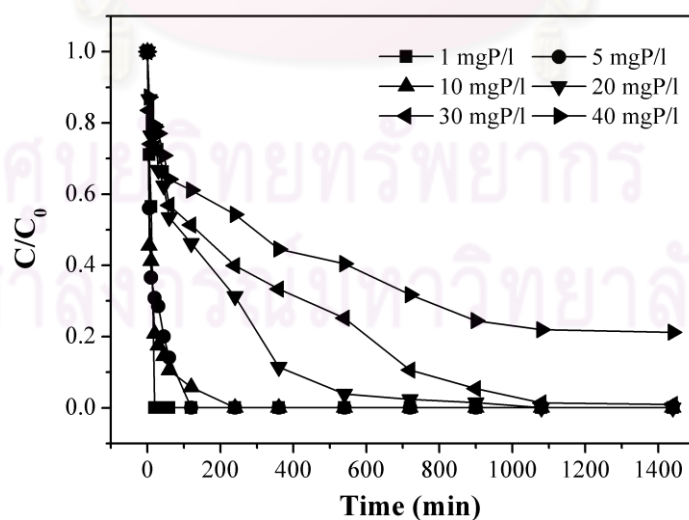


**Figure 1**  $C/C_0$  of phosphate using  $\text{Fe}_2\text{O}_3\text{-Mg-Al}$  LDHs as adsorption in terms of time and initial phosphate concentration.

**Table 2.**  $C/C_0$  of phosphate using Mg-Al LDHs in powder form as adsorption in terms of time and initial phosphate concentration

Time (min)	$C/C_0$					
	1 mg P/l	5 mg P/l	10 mg P/l	20 mg P/l	30 mg P/l	40 mg P/l
0	1	1	1	1	1	1
5	0.767	0.933	0.684	0.909	0.904	0.946
10	0.609	0.341	0.5295	0.923	0.837	0.880
20	0.010	0.205	0.382	0.774	0.788	0.841
30	0.005	0.159	0.290	0.707	0.731	0.786
45	0.005	0.0017	0.187	0.672	0.6813	0.752
60	0.005	0.0017	0.1163	0.557	0.609	0.696
120	0.005	0.0017	0.082	0.508	0.529	0.633
240	0.005	0.0017	0.0010	0.437	0.432	0.567
360	0.005	0.0017	0.0010	0.323	0.332	0.458
540	0.005	0.0017	0.0010	0.215	0.279	0.409
720	0.005	0.0017	0.0010	0.097	0.151	0.345
900	0.005	0.0017	0.0010	0.041	0.035	0.239
1080	0.005	0.0017	0.0010	0.026	0.014	0.216
1440	0.005	0.0017	0.0010	0.0004	0.010	0.213

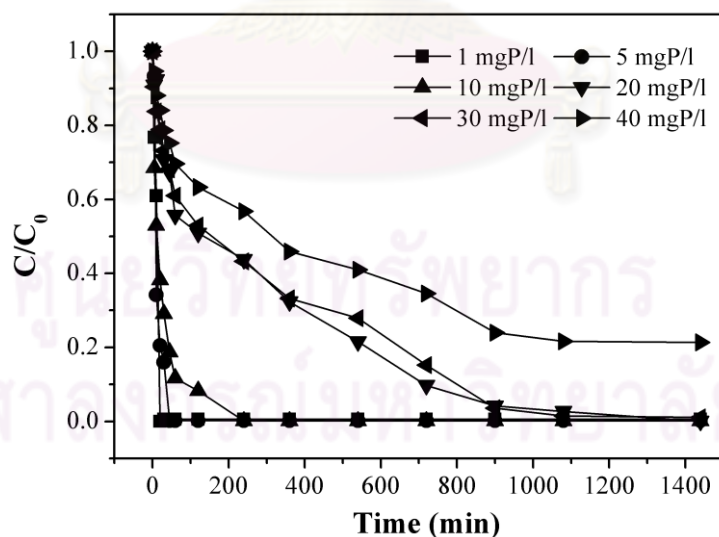


**Figure 2**  $C/C_0$  of phosphate using Mg-Al LDHs as adsorption in terms of time and initial phosphate concentration.

**Table 3** Adsorption capacity of  $\text{Fe}_2\text{O}_3\text{-Mg-Al}$  LDHs in powder form as function time and initial concentration

Time (min)	Adsorption capacity (mg/g)					
	1 mg P/l	5 mg P/l	10 mg P/l	20 mg P/l	30 mg P/l	40 mg P/l
0	0	0	0	0	0	0
5	0.477	2.254	5.66	2.94	5.15	5.109
10	0.718	3.2545	6.11	5.19	8.13	8.164
20	1.649	3.55	8.240	4.77	8.536	8.536
30	1.649	3.668	8.58	7.322	8.8	9.3
45	1.649	4.104	8.890	8.3	10.75	11.55
60	1.649	4.40	9.30	10.25	13.540	14.455
120	1.649	5.130	9.804	11.85	15.29	15.7455
240	1.649	5.130	10.408	15.140	18.87	18.5091
360	1.649	5.130	10.408	19.51	20.94	22.455
540	1.649	5.130	10.408	21.18	23.509	24.1
720	1.649	5.130	10.408	21.504	28.08	27.618
900	1.649	5.130	10.408	21.709	29.72	30.509
1080	1.649	5.130	10.408	22.030	30.98	31.6273
1440	1.649	5.130	10.408	22.0309	31.13	31.9045

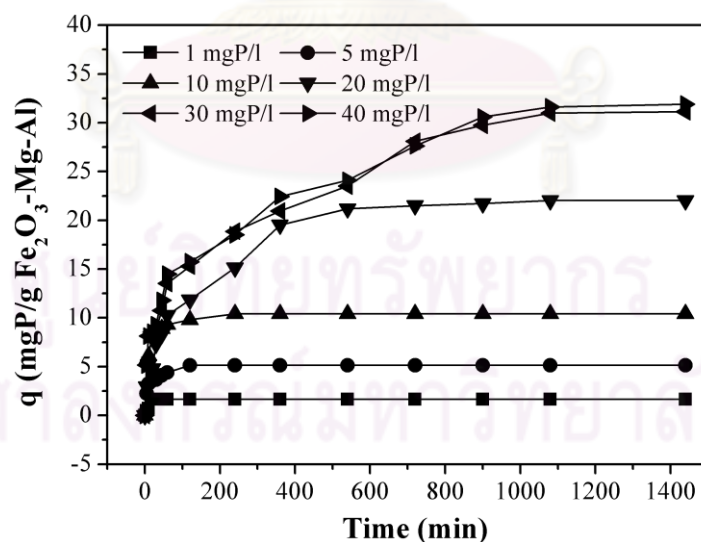
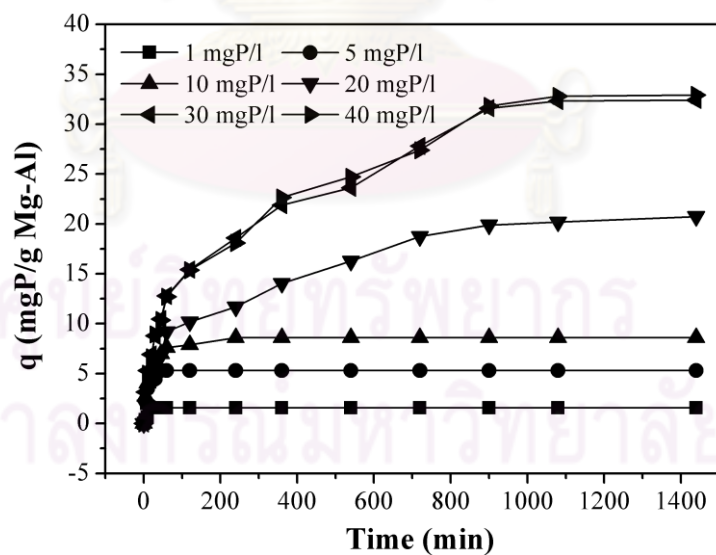


**Figure 3** Adsorption capacities of  $\text{Fe}_2\text{O}_3\text{-Mg-Al}$  LDHs.



**Table 4** Adsorption capacity ( $q$ ) of Mg-Al LDHs in powder form as function time and initial concentration

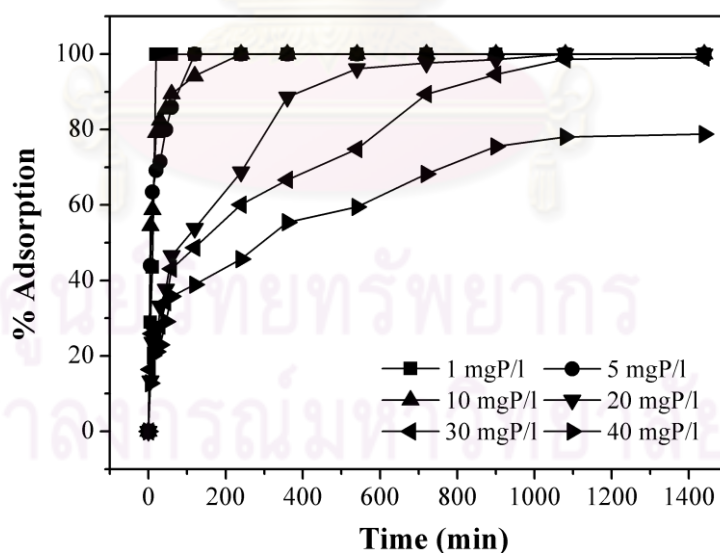
Time (min)	Adsorption capacity (mg /g)					
	1 mg P/l	5 mg P/l	10 mg P/l	20 mg P/l	30 mg P/l	40 mg P/l
0	0	0	0	0	0	0
5	0.368	0.354	2.713	1.877	3.145	2.236
10	0.61	3.5	4.05	1.586	5.313	4.99
20	1.581	4.22	5.32	4.681	6.92	6.65
30	1.57	4.468	6.109	6.07	8.79	8.927
45	1.57	5.309	7	6.8	10.45	10.36
60	1.57	5.309	7.60	9.186	12.79	12.7
120	1.57	5.309	7.9	10.1	15.431	15.36
240	1.57	5.309	8.604	11.66	18.6	18.1
360	1.57	5.309	8.604	14.03	21.88	22.65
540	1.57	5.309	8.604	16.27	23.62	24.71
720	1.57	5.309	8.604	18.73	27.79	27.39
900	1.57	5.309	8.604	19.88	31.6	31.827
1080	1.57	5.309	8.604	20.18	32.30	32.80
1440	1.57	5.309	8.604	20.736	32.41	32.91



**Figure 4** Adsorption capacities of Mg-Al LDHs.

**Table 5** Adsorption percentage of  $\text{Fe}_2\text{O}_3\text{-Mg-Al}$  LDHs in powder form as function time and initial concentration

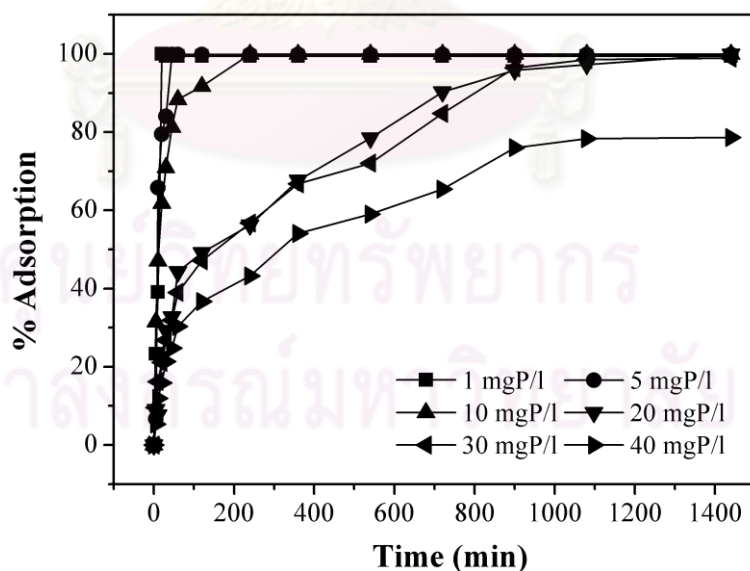
Time (min)	% Adsorption					
	1 mg P/l	5 mg P/l	10 mg P/l	20 mg P/l	30 mg P/l	40 mgP/l
0	0	0	0	0	0	0
5	28.92	43.93	54.45	13.36	16.42	12.735
10	43.52	63.42	58.73	23.58	25.90	20.090
20	99.94	69.18	79.17	21.68	27.17	21.072
30	99.94	71.48	82.48	33.24	28.01	22.957
45	99.94	79.98	85.41	37.67	34.21	29.118
60	99.94	85.92	89.43	46.52	43.09	35.783
120	99.94	99.98	94.19	53.80	48.66	38.868
240	99.94	99.98	99.99	68.72	60.069	45.69
360	99.94	99.98	99.99	88.57	66.66	55.408
540	99.94	99.98	99.99	96.14	74.82	59.492
720	99.94	99.98	99.99	97.60	89.39	68.21
900	99.94	99.98	99.99	98.53	94.61	75.516
1080	99.94	99.98	99.99	99.99	98.61	78.074
1440	99.94	99.98	99.99	99.99	99.08	78.758



**Figure 5** Adsorption percentages of  $\text{Fe}_2\text{O}_3\text{-Mg-Al}$  LDHs.

**Table 6** Adsorption percentage of Mg-Al LDHs in powder form as function time and initial concentration

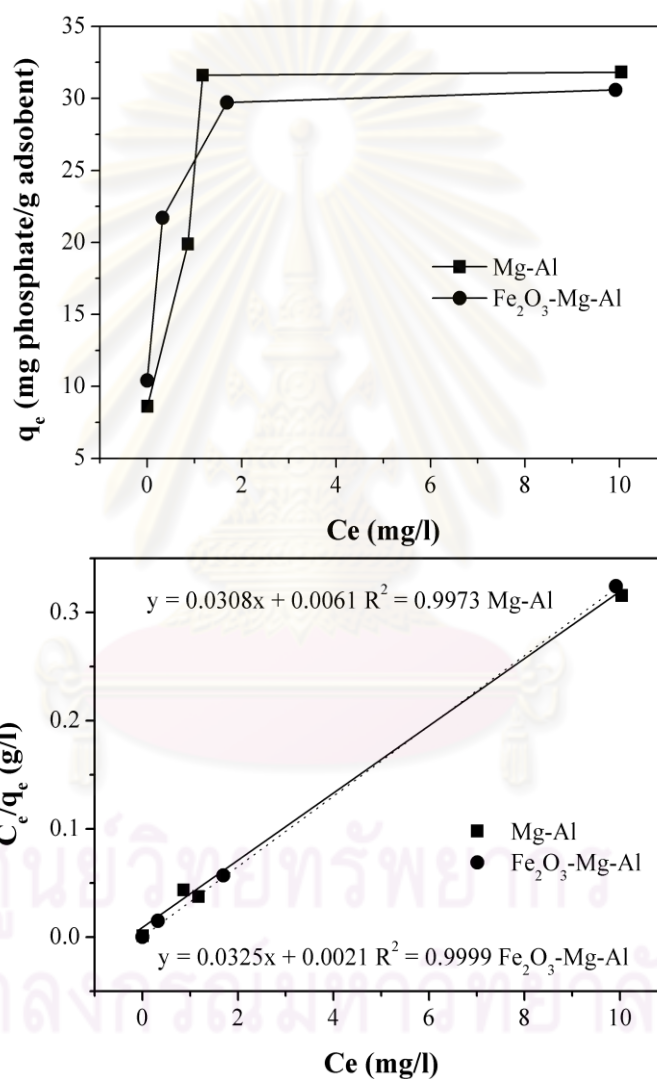
Time (min)	% Adsorption					
	1 mg P/l	5 mg P/l	10 mg P/l	20 mg P/l	30 mg P/l	40 mg P/l
0	0	0	0	0	0	0
5	23.27	6.66	31.50	9.04	9.60	5.341
10	39.08	65.81	47.01	7.64	16.21	11.93
20	99.00	79.48	61.79	22.56	21.12	15.883
30	99.42	84.01	70.92	29.27	26.82	21.322
45	99.4	99.82	81.26	32.77	31.89	24.753
60	99.4	99.8	88.33	44.28	39.02	30.33
120	99.4	99.8	91.71	49.12	47.08	36.69
240	99.4	99.8	99.89	56.24	56.74	43.23
360	99.4	99.8	99.89	67.65	66.77	54.12
540	99.4	99.8	99.89	78.46	72.07	59.02
720	99.4	99.8	99.89	90.29	84.80	65.432
900	99.4	99.8	99.89	95.83	96.40	76.01
1080	99.4	99.8	99.89	97.30	98.57	78.36
1440	99.4	99.8	99.89	99.95	98.90	78.62



**Figure 6** Adsorption percentages of Mg-Al LDHs.

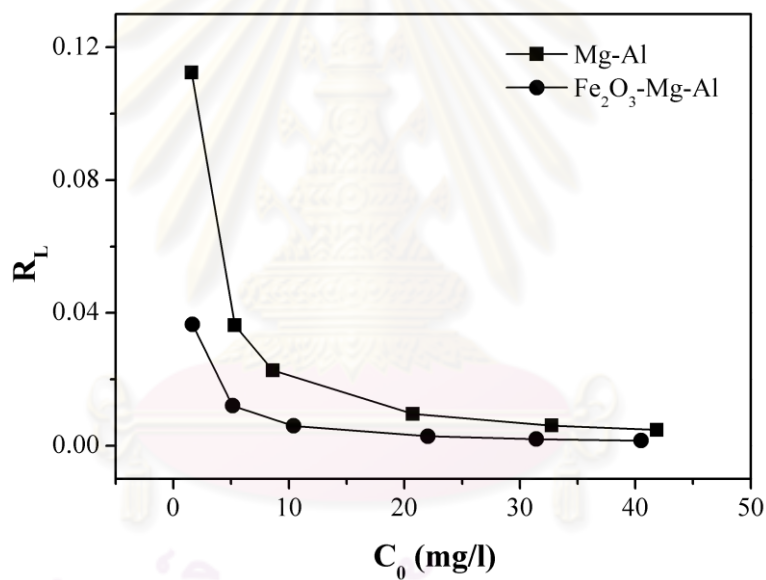
**Table 7** Langmuir adsorption isotherm of Fe<sub>2</sub>O<sub>3</sub>-Mg-Al LDHs and Mg-Al LDHs

PO <sub>4</sub> <sup>3-</sup> conc. (mg P/l)	C <sub>0</sub>		C <sub>e</sub>		(C <sub>0</sub> -C <sub>e</sub> )/M		C <sub>e</sub> /[(C <sub>0</sub> -C <sub>e</sub> )/M]	
	Fe- Mg-Al	Mg-Al	Fe- Mg-Al	Mg-Al	Fe- Mg-Al	Mg-Al	Fe-Mg- Al	Mg-Al
10	10.4	8.61	0.001	0.009	10.408	8.604	8.6E-5	0.001
20	22.0	20.7	0.32	0.8636	21.711	19.881	0.0147	0.043
30	31.4	32.7	1.69	3	29.728	29.77	0.0568	0.100
40	40.5	41.86	9.918	10.04	30.59	31.82	0.324	0.315

**Figure 7** Linear plot of Langmuir adsorption isotherm of phosphate on Fe<sub>2</sub>O<sub>3</sub>-Mg-Al LDHs and Mg-Al LDHs.

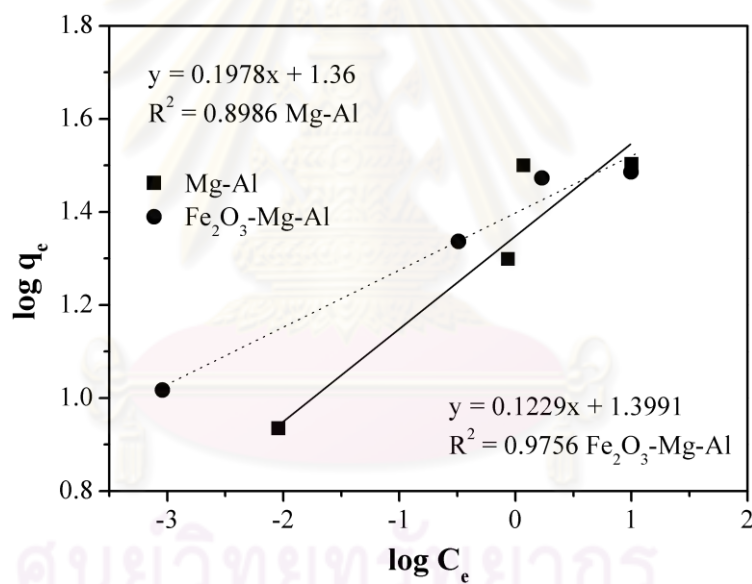
**Table 8** Separate factor ( $R_L$ )

$\text{PO}_4^{3-}$ conc. (mg P/l)	$C_0$		b		$R_L$	
	Fe-Mg-Al	Mg-Al	Fe-Mg-Al	Mg-Al	Fe-Mg-Al	Mg-Al
1	1.65	1.58	16	5	0.012	0.036
5	5.1318	5.318	16	5	0.005	0.0226
10	10.409	8.613	16	5	0.002	0.009
20	22.031	20.745	16	5	0.001	0.006
30	31.418	32.77	16	5	0.001	0.004
40	40.509	41.86	16	5	0.036	0.112

**Figure 8** Separate factors ( $R_L$ ).

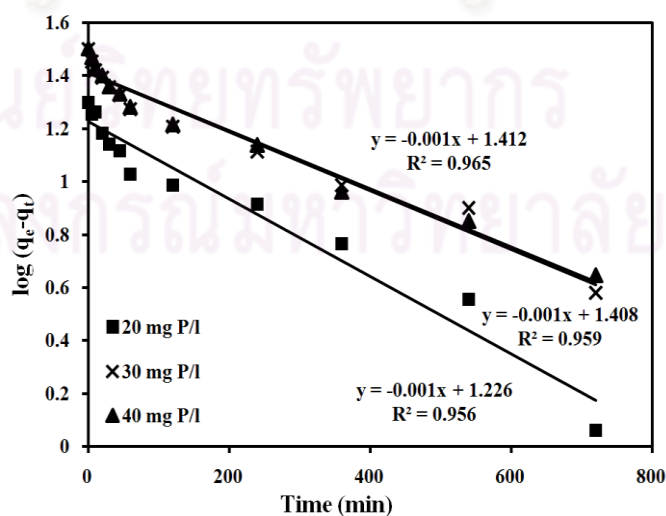
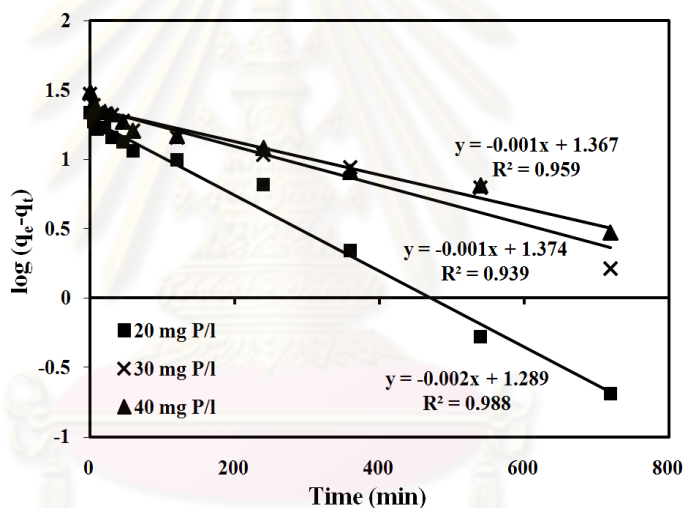
**Table 9** Freundlich adsorption isotherm of Mg-Al LDHs

conc. (mg P/l)	log $q_e$		log $C_e$	
	Fe-Mg-Al	Mg-Al	Fe-Mg-Al	Mg-Al
1	0.21724	0.1961	-3.04575	-2.0457
5	0.7101	0.7250	-3.04575	-2.0457
10	1.0173	0.9347	-3.045757	-2.0457
20	1.3366	1.2984	-0.49485	-0.0636
30	1.4731	1.4737	0.227886	0.4771
40	1.4855	1.5027	0.9964320	1.0017

**Figure 9** Linear plots of Freundlich adsorption isotherm of  $Fe_2O_3$ -Mg-Al LDHs and Mg-Al LDHs.

**Table 10** Pseudo-first-order and pseudo-second-order kinetic constants

Adsorbent	Initial $\text{PO}_4^{3-}$ conc. (mg P/l)	Pseudo-first-order			Pseudo-second-order		
		$q_e$ (mg/g)	$k_1 \times 10^{-3}$ ( $\text{min}^{-1}$ )	$R^2$	$q_e$ (mg/g)	$k_2 \times 10^{-4}$ (mg/g min)	$R^2$
$\text{Fe}_2\text{O}_3$ - Mg-Al	20	19.45	-4.60	0.99	23.81	5.680	0.99
	30	23.66	-2.30	0.94	33.33	2.946	0.98
Mg-Al	20	16.83	-2.30	0.96	22.22	3.741	0.99
	30	25.59	-2.30	0.96	34.48	2.441	0.98
	40	25.82	-2.30	0.97	35.71	2.200	0.98

**Figure 10a** Linear plot of pseudo-first-order kinetic model for phosphate adsorption on  $\text{Fe}_2\text{O}_3$ -Mg-Al LDHs and Mg-Al LDHs.

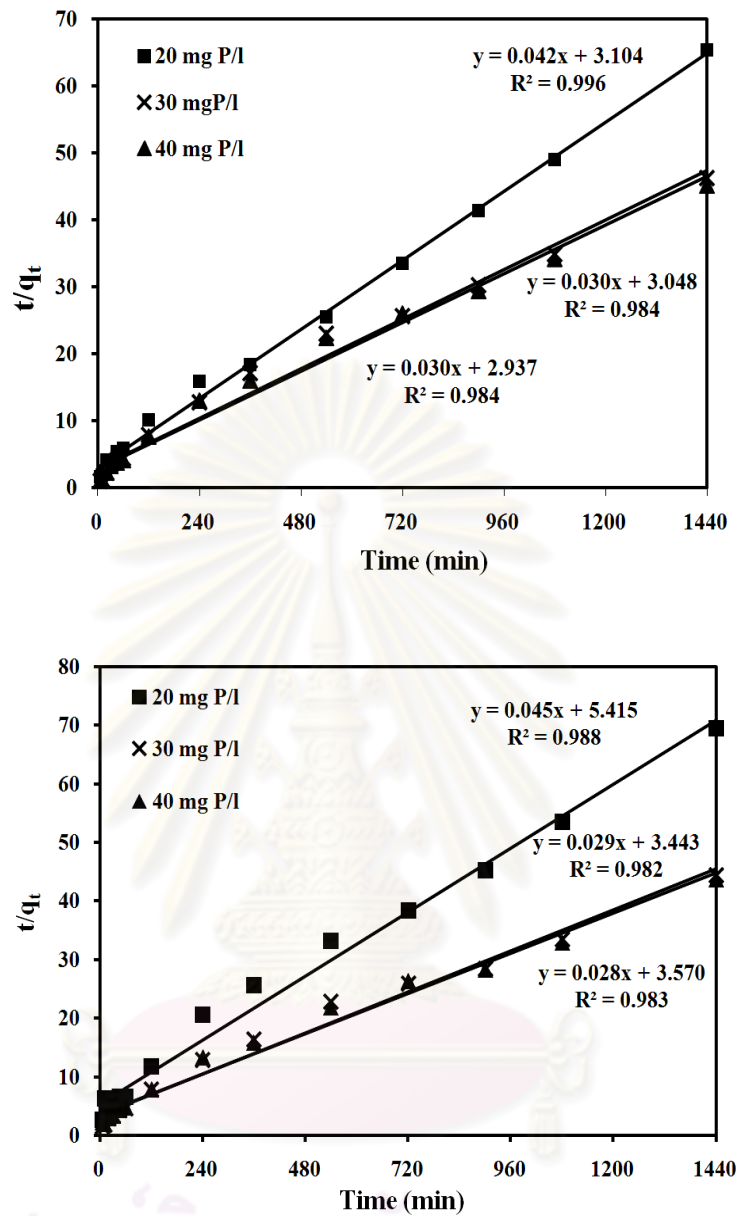


**Figure 10b** Linear plot of pseudo-second-order kinetic model for phosphate adsorption on Fe<sub>2</sub>O<sub>3</sub>-Mg-Al LDHs and Mg-Al LDHs.



**Table 11** Concentration of phosphate using granulated form by mechanical coating technique at 5 mg P/l over time

Time(min)	Phosphate concentration (mg/l)		
	Fe <sub>2</sub> O <sub>3</sub> -Mg-Al	Mg-Al	Alumina ball
0	6.304545	6.072727	5.263636
5	3.863636	4.454545	1.768182
10	3.20098	2.268182	1.590909
20	2.790909	2.463636	1.027273
30	3.131818	1.927273	1.472727
45	0.904545	1.254545	1.436364
60	0.863636	0.963636	0.809091
120	0.259091	0.559091	0.595455
240	0.077273	0.559091	0.377273
360	0.077273	0.559091	0.231818
540	0.077273	0.559091	0.181818
720	0.077273	0.559091	0.186364
900	0.077273	0.559091	0.177273
1080	0.077273	0.559091	0.177273
1440	0.077273	0.559091	0.176818

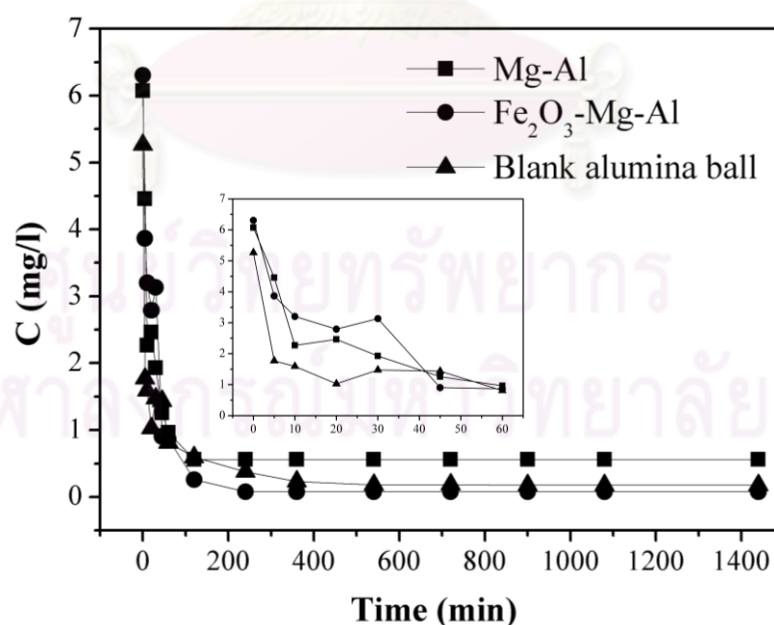


**Figure 11** Concentrations of phosphate using granulated form by mechanical coating technique over time.

**Table 12** Concentration of phosphate using granulated form by extrusion technique at 5 mg P/l over time

Time(min)	Phosphate concentration (mg /l)	
	Fe <sub>2</sub> O <sub>3</sub> -Mg-Al	Mg-Al
0	6.004545	6.381818
5	5.8564	5.972727
10	5.036364	4.918182
20	4.727273	5.322727
30	5.377273	5.340909
45	5.295455	4.736364
60	4.763636	5.031818
120	4.668182	4.286364
240	4.627273	3.381818
360	3.909091	2.80989
540	3.818182	1.513636
720	3.627273	1.363636
900	2.372727	1.490909
1080	1.518182	1.490909
1440	1.518182	1.490909

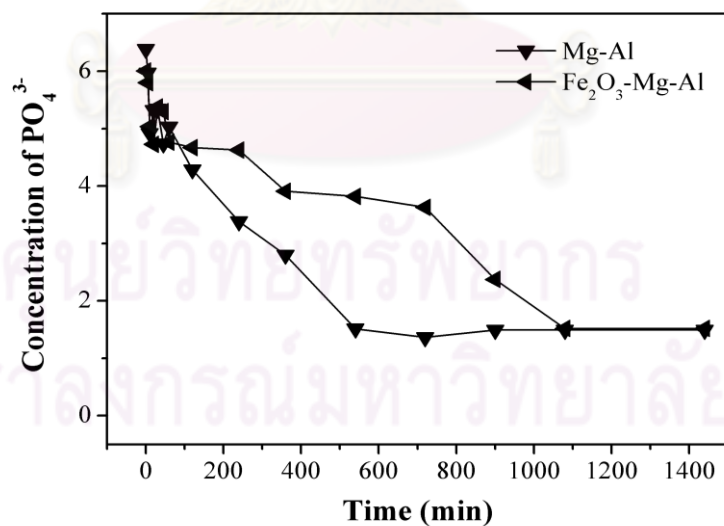


**Figure 12** Concentrations of phosphate using granulated form by extrusion technique over time.

**Table 13** Percentage of adsorption of phosphate using granulated form by mechanical coating and extrusion technique at 5 mg P/l over time

Time(min)	% Adsorption				
	Mechanical coating			Extrusion	
	Fe <sub>2</sub> O <sub>3</sub> -Mg-Al	Mg-Al	Alumina ball	Fe <sub>2</sub> O <sub>3</sub> -Mg-Al	Mg-Al-
0	0	0	0	0	0
5	38.71	26.641	66.407	3.20	6.41
10	49.24	62.64	69.77	15.17	22.93
20	55.73	59.43	80.48	20.01	16.59
30	50.32	68.26	72.02	9.82	16.31
45	85.65	79.34	72.71	11.11	25.78
60	86.30	84.131	84.62	19.44	21.15
120	95.89	90.79	88.68	20.94	32.83
240	98.77	90.79	92.83	21.5	47.00
360	98.77	90.79	95.59	32.83	56.12
540	98.77	90.79	96.54	34.25	76.28
720	98.77	90.79	96.45	37.25	78.63
900	98.77	90.79	96.63	56.90	76.63
1080	98.77	90.79	96.63	70.29	76.63
1440	98.77	90.79	96.64	70.29	76.63

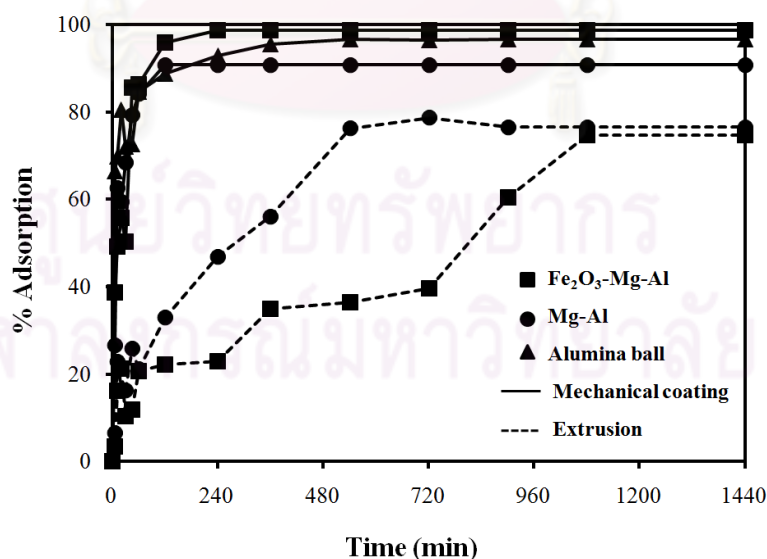


**Figure 13** Percentage of adsorption of phosphate using mechanical coating and extrusion techniques.

## BIOGRAPHY

- Name:** Miss Chanyarak Watthanachai
- Date of Birth:** August 5, 1986
- Nationality:** Thai
- Education:** 2005 - 2008, Bachelor Degree of Environmental Science, Faculty of Science, Silpakorn University
- Conference:** The 17<sup>th</sup> Regional Symposium on Chemical Engineering (RSCE 2010) at Bangkok, Thailand and the 5<sup>th</sup> International Conference on Advanced Materials and Nanotechnology (AMN-5) at Wellington, New Zealand in topic of synthesis and characterization of Fe<sub>2</sub>O<sub>3</sub>-Mg-Al supported beads for phosphate removal.



ศูนย์วิทยทรัพยากร  
จุฬาลงกรณ์มหาวิทยาลัย